A Comprehensive review on Advancements in Evaluation techniques for characterization of metallic nanoparticles.

Adnan Siddique Rehmatullah, Dr Geeta Bhagwat

HK college of Pharmacy, Mumbai Maharashtra.
HK College of Pharmacy,Mumbai Maharashtra.

ABSTRACT

Metallic nanoparticles have fascinated scientists for over a century because of their huge potential in nanotechnology. Today, these materials can be synthesized and modified with various structures which allow them to be applied widely in numerous branches of science. Nanomaterials could be single or multiple metals and have copious kinds of size, shape, and structure and, thus, lead to profusely beneficial properties. Understanding nanoparticle characteristics helps in validating the synthesis, deciphering the morphology evolution, improving the synthesis protocols, and comprehending the potential applications of nanoparticles. In the present review complete discussion has been done on the different characterization techniques which are used for the evaluation of metallic nanoparticles such TEM, SEM, NMR and DLS

KEYWORDS:-METALLIC NANOPARTICLE, CHARACTERIZATION TECHNIQUE, AND NMR.

I. INTRODUCTION

Nanotechnology, a science that deals preparation of nano-size particles ranging from 1 to 100 nm employing diverse synthesis strategies, and particle structure and size modification. The use of nanoparticles indifferent fields like molecular biology, physics, organic and inorganic chemistry, medicine and material science is unexpectedly augmented nowadays [1]Decrease in particle size to nano-size demonstrates peculiar and improved properties such as particle size distribution and morphology, which is not showed by larger particles of bulk material[2]The term 'nanoparticle' was coined from Greek work 'nano' that means 'dwarf or small' and when used as prefix it indicates size 10−9 one billionth of meter is equals to 1 nm [3]. Nanoparticles have both solute and separate particle phase properties. The surface to volume ratio of nanoparticle is 35–45% times higher as compared to large particle or atom. This unique extrinsic property of specific surface area of nanoparticle is a contributory factor for its high value and also influences different intrinsic properties such as strong surface reactivity which is size dependent [4]. Overall, these exclusive features of nanoparticles are responsible for its multifunctional properties and developing interest for its application in various fields like energy, medicines and nutrition [5]. Metallic nanoparticles or metal nanoparticles, a new terminology has been originated in the field of nanoparticles in recent few years. The noble metal like gold, silver, and platinum having beneficialeffects on health are utilized for the synthesis of nanoparticles and designated as metallic nanoparticles [6]. Nowadays researchers are focusing on metal nanoparticles, nanostructures and nanomaterial synthesis because of their conspicuous properties that are useful for catalysis[7], composite like polymer preparations [8],disease diagnosis and treatment , sensor technology [9,10]and labelling of optoelectronic recorded media [11]. Different physical and chemical methods such as electrochemical changes, chemical reduction, and photochemical reduction are commonly employed for the preparation and stabilization of metallic nanoparticles[12,13].The selection of preparation method of metallic nanoparticle is equally important because during nanoparticle synthesis processes such as kinetics of interaction of metal ions with reducing agent, adsorption process of stabilizing agent with metal nanoparticles and various experimental techniques produces strong influence on its morphology (structure and size) stability and physicochemical properties[14]. Many metal particles present in the products such as cosmetic products, detergents, tooth paste, soaps, shampoos, medicines and pharmaceutical products are directly coming in contact with human. Gold is widely used in the medicines and Ayurvedic preparations in India and China [6]. Gold nanoparticles are employed for many diagnostic and drug delivery purposes [15]. Apart from this, other metal nanoparticles like silver nanoparticles are also employed for various biomedical applications such as separation science [16]and novel drug delivery system . Silver is well

known for its antimicrobial and inflammatory potential. This property is selectively used to elevate faster wound healing and commercially adopted in wound dressing, different pharmaceutical dosage formulation and medical implant coating. Other metal nanoparticles like platinum nanoparticles also evaluated for their health beneficialeffect and successfully used in biomedical applications in either pure form or metal alloyed as a single or in combination with other metal nanoparticles. The use of metal nanoparticles is continuously increasing worldwide in biomedicine and allied disciplines [17,18]. In view of this, present review is an assortment of various methods used for the preparation of metallic

nanoparticles, their advantages, disadvantages and applications.

Divers methods are employed for the metallic nanoparticles preparation which are categorized into two main types as bottom up methods and top down methods, and enlisted in Table 1 [19]

The principal difference between both the methods is starting material of nanoparticle preparation. Bulk material is used as starting material in top-down methods and particle size is reduced to nanoparticles by different physical, chemical and mechanical processes, whereas atoms or molecules are the starting material in bottom up methods (Fig. 1).
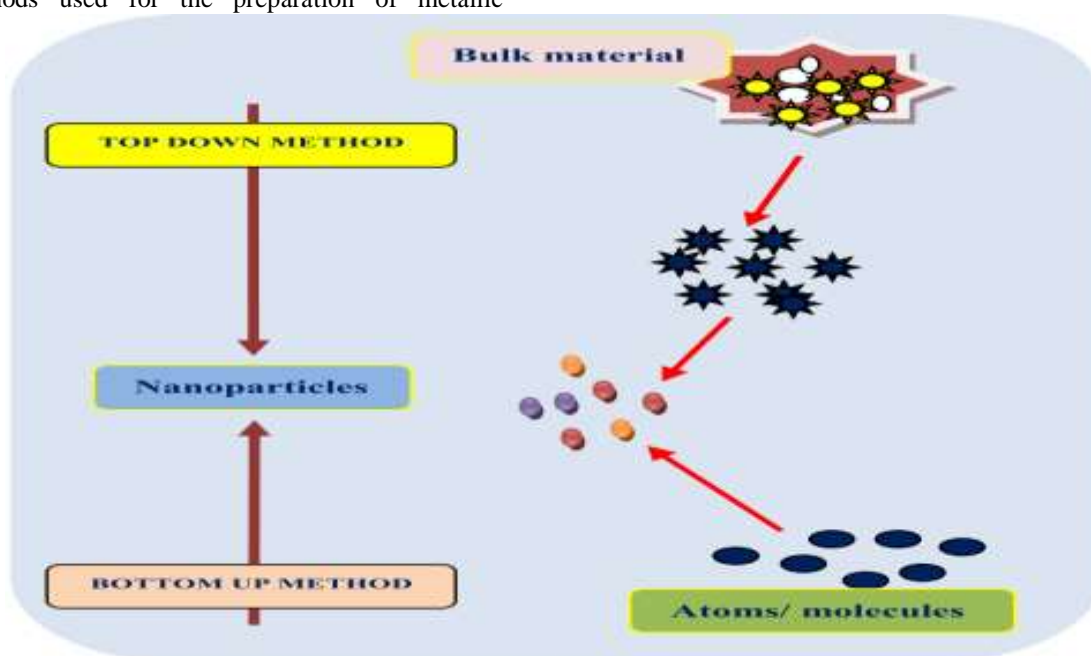
Fig 1 an overview of top down and bottom up method

Srno	Top down method		Bottom up method	
1	Method	Example	Method	Example
2	Mechanical milling	Ball milling Mechanochemical method	Solid state methods	Physical vapor deposition Chemical vapor deposition

3	Laser ablation		Liquid state synthesis methods	Sol gel methods Chemical reduction Hydrothermal method
4	Sputtering		Gas phase methods	Spray pyrolysis Laser ablation Flame pyrolysis
5			Biological method	Bacteria Fungus Yeast Algae Plant extract
6			Other methods	Electrodeposition process Microwave technique Supercritical fluid precipitation process Ultra sound technique

II. INTRODUCTION TO EVALUATION TECHNIQUE.

Nanoscale materials often present properties different from their bulk counterparts, as their high surface results in an exponential increase of the reactivity at the molecular level. Such properties include electronic, optical and chemical properties, while the mechanical characteristics of the nanoparticles (Metallic-NPs) may also differ extensively[20].This enables them to be an object of intensive studies due to their academic interest and the prospective technological applications in various fields. Such nanostructures may be synthesized by a wide number of methods, which involve mechanical, chemical and other pathways [21]. Nowadays, many more types of nanomaterials are synthesized than only a decade ago, and in higher amounts than before, requiring the development of more precise and credible protocols for their characterization. However, such characterization is sometimes incomplete. This is because of the inherent difficulties of nanoscale materials to be properly analysed, compared to the bulk materials (e.g. too small size and low quantity in some cases following laboratory-scale production). In addition, the multidisciplinary aspects of nanoscience and nanotechnology do not permit every research team to have easy access to a broad range of characterization facilities. In fact, quite often a wider characterization of Metallic-NPs is necessary, requiring a comprehensive approach, by combining techniques in a complementary way. In this context, it is desirable to know the limitations and strengths of the different techniques, in order to know if in some cases the use of only one or two of them is enough to provide reliable information when studying a specific parameter (e.g. particle size). Nanoscience and nanotechnology are still undergoing constant growth, and the scientific community is rather aware that there may be certain differences between the way analytical characterization methods operate for nanomaterials, in comparison with their more 'traditional' modes of use for more 'conventional' (macroscopic) materials.[22]

Herein we describe extensively the use of different methods for the characterization of metallic-NPs. These techniques are sometimes exclusive for the study of a particular property, while in other cases they are combined.[23].There are Spectroscopy based techniques like e.g.(UV,FTIR,ICP) which provide information on the Surface plasmon resonance of the metals also give information on the concentration and yield. There are microscopy-based techniques (e.g. TEM, HRTEM, and AFM – the full names of the techniques are provided later in the text, when presenting each one of them), Many other techniques provide further information on the structure, elemental composition, optical properties and other common and more specific physical properties of the nanoparticle samples. Examples of these techniques include X-ray, spectroscopy and scattering techniques.

This review is organized in different sections, which will present numerous distinct characterization techniques for Metallic-NPs in relation to the properties studied (see Tables 1 and 2). The sections are categorized according to the different technique groups, as described above.-

Table 1 Summary of the experimental techniques that are used for metallic nanoparticle characterization featured in this paper

Section	Technique	Main information derived
1	UV-Vis	Optical properties, size, concentration, agglomeration state, hints on NP shape
2	FTIR	Surface composition, ligand binding
3	NMR (all types)	Ligand density and arrangement, electronic core structure, atomic composition, influence of ligands on NP shape, NP size
4	ICP-MS	Elemental composition, size, size distribution, NP concentration
4.1 to 4.5	SIMS, ToF-SIMS, MALDI	Chemical information (surface-sensitive) on functional group, molecular orientation and conformation, surface topography, MALDI for NP size
5 and 6	ICP-AES and ICP-OES	Concentration
7 and 8	DLS and NTA	DLS Hydrodynamic size, detection of agglomerates
9 and 10	pH and zeta potential	Stability information
11	XRD (group: X-ray based techniques)	Crystal structure, composition, crystalline grain size
11.1 to 11.5	XAS (EXAFS, XANES) X-ray absorption coefficient (element-specific) .	chemical state of species, interatomic distances, Debye–Waller factors, also for non-crystalline NPs. SAXS Particle size, size distribution, growth kinetics XPS Electronic structure, elemental composition, oxidation states, ligand binding (Surface-sensitive).
12.1 to 12.8	TEM, HRTEM,AFM,SEM	NP size, size monodispersity, shape, aggregation state, detect and localize/ quantify Metallic-NPs in matrices, study growth kinetics

Table 2:- Parameters needed to be determined and the corresponding characterization techniques

Entity characterized	Characterization techniques suitable
Size (structural properties)	TEM, XRD, DLS, NTA, SAXS, HRTEM, SEM, AFM, EXAFS, FMR, DCS, ICP-MS, UV-Vis, MALDI, NMR,
Shape	TEM, HRTEM, AFM, EPLS, FMR, 3D-tomography
Elemental-chemical composition	XRD, XPS, ICP-MS, ICP-OES, SEM-EDX, NMR
Crystal structure	XRD, EXAFS, HRTEM, electron diffraction, STEM
Size distribution	DCS, DLS, SAXS, NTA, ICP-MS, FMR, DTA, , SEM
Ligand	XPS, FTIR, NMR, SIMS, FMR, TGA, SANS

binding/composition/density/arrangement/mass, surface composition	
Optical properties	UV-Vis-NIR, PL, EELS-STEM
Concentration	ICP-MS, UV-Vis
Surface charge	Zeta potential

1. UV-VIS SPECTROSCOPY (UV-VIS)

UV-Vis spectroscopy is relatively facile and low-cost characterization method that is often used for the study of nanoscale materials. It measures the intensity of light reflected from a sample and compares it to the intensity of light reflected from a reference material. Metallic-NPs have optical properties that are sensitive to size, shape, concentration, agglomeration state and refractive index near the NP surface, which makes UV-Vis spectroscopy an important tool to identify, characterize and investigate these materials, and evaluate the stability of metallic NP colloidal solutions.[24]Gold, silver and copper nanostructure sols exhibit characteristic UV-Vis extinction spectra due to the existence of a LSPR signal in the visible part of the spectrum. In certain cases (e.g. metal chalcogenide Metallic-NPs and anisotropic gold or silver nanostructures), Local surface plasmon resonance (LSPR) bands at the near-infrared (NIR) wavelength region can also appear.151 Besides characterizing the metallic NP optical properties, the size and molar concentration of zerovalent Au, for example, can also be obtained from the UV-Vis measurements. For this calculation, which can also be performed in situ under certain conditions, the position of the LSPR and the extinction at this wavelength, as well as the ratio of extinctions at the wavelength of the LSPR and at 450 nm (ALSPR/A450), are needed.[25]The absorbance at 350–400 nm wavelengths can also be used to measure the gold colloid concentration, however with an uncertainty up to 20–30% due to a rather slight influence of parameters such as NP size, surface modification and oxidation state. If these factors are taken into account upon calculation, the uncertainty in determining the Au NP concentration can be decreased extensively.[25]In fact, the maximum absorbance at the UV-Vis spectra has also been successfully used for the calculation of the concentration of citrate-coated silver Metallic-NPs.[26]Haiss et al. have published a very high profile study on the utility of UV-Vis spectra to determine the size and concentration of Au Metallic-NPs.[27]The colloidal stability of Au Metallic-NPs can be quantitatively characterized by UV-Vis absorbance spectroscopy, as shown by Pennathur and colleagues. Particle instability parameter (PIP) is a universal technique to quantitatively characterize the stability of plasmonic nanomaterials based on UV-Vis absorbance spectroscopy that does not depend on the colloid system and can fully record the evolution of a given studied system over time. It is a robust and generalizable approach, not only for Au Metallic-NPs, but also for plasmonic Metallic-NPs as a whole.[28]. Overall, this method can be considered low-cost, non-destructive and quick for the recognition of metallic NP systems and types. Ag nanostructures have also been extensively studied by UV-Vis spectroscopy. Jha and co-workers investigated the influence of maturing time and concentration of NaBH4 on size with UV-Vis. Their method, under the framework of the Mie theory, was employed to determine the particle size and size distribution. In fact, the LSPR of Metallic-NPs is affected by size, shape, interparticle interactions, free electron density and surrounding medium, and this helps to obtain a screening of the electron injection and aggregation of Metallic-NPs. In this way, it was possible to characterize the Ag NP formation kinetics and the final colloidal stability.[29]In another work, Ag Metallic-NPs were prepared via a green synthesis involving the flowers of the Moringa oleifera (MO) plant. This plant acted as a reducing and stabilizing agent, and the resulting particles were studied by FTIR, UV-Vis and other techniques. FTIR experiments demonstrated that proteins in the MO flower extract were adsorbed on Ag Metallic-NPs, acting as capping agents. It also indicated that retinoic acid, a component of the MO flower extract, acted as a reductant. UV-Vis analysis verified the existence of LSPR in the produced particles and as the concentration of the MO flower extract increased, the absorption spectra showed a blue shift with decreasing NP size.[30]

2. FOURIER TRANSFORMS INFRARED SPECTROSCOPY (FTIR)

FTIR is a technique based on the measurement of the absorption of electromagnetic radiation with wavelengths within the mid-infrared region (4000–400 cm^{-1}). If a molecule absorbs IR radiation, the dipole moment is somehow modified and the molecule becomes IR active. A recorded

spectrum gives the position of bands related to the strength and nature of bonds, and specific functional groups, providing thus information concerning molecular structures and interactions.[31]

The purpose of FTIR analysis in synthesis of metallic nanoparticle is that if a metallic nanoparticle is synthesized via green method where the use of plant extract is done in such cases to identify what group of the plant extract was involved in reducing the metal ions to metallic nanoparticles and to identify which groups are adsorbed on to the surface of the metallic nanoparticle as a capping agent

For example baker syed et.al carried out the synthesis of bimatllic silver and gold nanoparticles using the plant extract of Annona squamosa to find out the possible role of phyto-components in mediating the synthesis author further done the FTIR analysis.The possible role of Phyto-components present in aqueous plant extract responsible for mediating and stabilizing the nanoparticles was depicted using FTIR analysis. Perusal of scientific studies report FTIR as one of the ideal tool to predict the functional moieties. In the present investigation, vibrational stretch occurring at 3339 corresponds to NH stretching, 1638 corresponds to C@C stretching and 663 corresponds to C-OH .Scientific studies on FTIR analysis of plant mediated nanoparticles reports that different functional moieties like hydroxyl, carboxyl and amide are responsible for reduction of metal ions to produce nanoparticles Interestingly, in plant-mediated synthesis of nanoparticles, the phyto-components also play important role in stabilization of nanoparticles which is very crucial for rendering its applicative properties. These results also coincide with reports of earlierfindings [32]

III. NUCLEAR MAGNETIC RESONANCE (NMR) SPECTROSCOPY

NMR Spectroscopy is another important analytical technique in the quantitative and structural determination of Nano scale materials. It is based on the NMR phenomenon exhibited by nuclei that possess non-zero spin when placed in a strong magnetic field, which causes a small energy difference between the 'spin-up' and 'spin-down' states. Transitions between these states can be probed by electromagnetic radiation in the radio wave range. NMR is typically used to study the interactions or coordination between the ligand and the surface of diamagnetic or antiferromagnetic

NPs. It is, however, not suitable to characterize ferric- or ferromagnetic materials, as the large saturation magnetization of such materials causes variations in a local magnetic field, which lead to shifts of the signal frequency and dramatic decreases in relaxation times. As a result, significant broadening of the signal peaks occurs, making the measurements practically inutile and unable to be interpreted.[66] Marbella and Millstone have written a comprehensive review article on the NMR techniques for noble Metallic-NPs. NMR spectroscopy can help toward the routine, straightforward, molecular-scale investigation of NP formation and morphology in situ, in both solution and solid phase. It is particularly useful for analysing both the formation and final architecture of noble metal Metallic-NPs. The capping ligands are also typically studied by NMR, and such measurements can yield information on the properties of the particle core (e.g. electronic structure, atomic composition, or compositional architecture). Insights into ligand density, arrangement and dynamics can also be derived.[102] besides facilitating the monitoring of the chemical evolution of ligand precursors and their role in particle growth, NMR is also employed to probe the role of capping ligands for the determination of particle shape. Overall, NMR can screen the chemical conversion of NP precursors in both the solution and solid phase, with high spatial and chemical resolution, under distinct reaction conditions, and for diverse metal identities; this helps in the better comprehension of the reaction mechanisms for NP synthesis. Moreover, NMR is useful for the monitoring of the process and final products of ligand exchange, when the initial capping ligands need to be replaced.[33]

2.1. 1H NMR

The 1 H NMR chemical shift behaviour is sensitive to the surrounding electronic environment; this includes the electronic structures and bonding environment of the nucleus. Consequently, any changes in the handedness of a molecule can be 'felt' by neighboring spin positions and observed as changes in chemical shift. This renders NMR significant to assess the chirality or absence of chirality of small, moleculelike nanoclusters. NMR can also be applied for the direct monitoring of the diffusion of adsorbed gases onto the surface of Metallic-NPs. Finally, NMR is utile for the measurement of the hydrodynamic radius of Metallic-NPs and thus constitutes an important complement to more standard NP sizing techniques, such as TEM and DLS. Similar to DLS, NMR spectra are used to

define the NP size via the analysis of particle diffusion. In particular, NMR helps to extract the diffusion coefficient of well-dispersed species in solution diffusing according to Brownian motion only. Then the hydrodynamic size can be calculated through a rearrangement of the Stokes– Einstein equation.[33]Finally, a phenomenon known as 'Knight shift', which is induced by some metals and can be present upon NMR measurements, is also described in ref. 102. It has to be noted that the particle size, which can be safely analysed by NMR, can exceed by far the 100 nm in the case of polymerhybrid particles,[34,35]whereas metallic-NPs have to be at around the size range of 1–5 nm in order to acquire meaningful NMR measurements. 1 H solution NMR has been reviewed by Hens and Martins as a tool for the investigation of the surface chemistry of colloidal Metallic-NPs.[36]

2.2. DIFFUSION-ORDERED NMR

DOSY-NMR offers the possibility to distinguish in situ free ligands from bound ligands, while the distribution of these species can also be quantified. Solution NMR can be employed to identify tightly bound ligands and quantify their surface density of sterically stabilized colloidal Metallic-NPs.[36]Jicsinszky and co-workers studied hydrophilic heptakis(6-deoxy-6-thio)cyclomaltoheptose capped Au Metallic-NPs with DOSY-NMR. This technique proved to be an effective, reliable and rapid way to investigate the role of the total concentration of gold in solvated metal atom (SMA) solutions as well as of the Au/capping ligand molar ratio on NP sizes. NMR measurements also helped to acquire some basic information on the drug transport and release capabilities of Au Metallic-NPs. This was achieved through the analysis of the nature of supramolecular aggregation processes and the ability of (Au)n/β-CDSH nanoaggregates to act as hosts for deoxycytidine (DC).[37]DOSY-NMR has also been employed to determine the nanoparticle size, e.g. in the case of Au Metallic-NPs prepared by Canzi et al. This was achieved by analysing the 1 H spectrum of the protecting ligands using 2D DOSY NMR, a method that could be facilely adapted also for other metal and semiconductor nanocrystals. Size estimates were acquired by using diffusion coefficient ratios derived from the proton signals from the alkyl thiolate groups bound to Au Metallic-NPs and a ferrocene internal standard. The authors stated that DOSY NMR was a reliable alternative method to calculate the NP size, being quicker and more cost-effective than TEM.[38]Coelho and colleagues used NMR spectroscopy to determine particular intermolecular

interactions and mechanisms of drug immobilization and location into surface PEG-modified Au Metallic-NPs. The authors highlighted the advantages of NMR as a non-destructive, highly reproducible method, sensitive to the structural details of molecules and molecular conjugates, which could be employed for both qualitative and quantitative characterization. Information of size, shape, dynamics, chemical structure, intermolecular interactions, and binding and exchange processes in complex nano-systems could be obtained.[39]The combined use of NMR with FTIR, UV-Vis, DLS and TEM could yield significant insights regarding important physicochemical properties of drug delivery systems, which influence their therapeutic efficacy.[39]

2.3. DEUTERIUM (2 H) NMR

Deuterium (2 H) NMR was employed to study the intramolecular ligand dynamics in d15-(PPh3)-capped Au Metallic-NPs. The authors made use of the ability of NMR to probe ligand structures and surface binding properties on Metallic-NPs by the in situ analysis of chemical shifts and resonance lines in the solid and liquid states. A specific feature of 2 H NMR is its simplicity and the capacity to distinguish the type of dynamics in amorphous and crystalline domains, for organic compounds that are isotopically labelled with deuterons.[40]Smith et al. used NMR to investigate the extent of ligand exchange between distinct kinds of thiolated molecules on the surface of Au Metallic-NPs. In particular, they determined ligand density values for single-moiety ligand shells and then used these data to describe the ligand exchange behaviour with a second, thiolated molecule.[41]Triphenylphosphine-capped 1.8 nm Au Metallic-NPs have been characterized by multinuclear NMR to investigate their surface structure and ligand binding environment. In solution, the ligand exchange kinetic reactions were screened by 1 H, 2 H and 31P NMR to analyse the exchange process.[42]Doyen et al. used UV-Vis and NMR to study the formation of Au Metallic-NPs by the citrate reduction method. 1D–1 H and DOSY-NMR measurements showed that citrate aggregates with Au(I) and Au(0) were formed. That work suggested that citrate, apart from being the reductant and the stabilizing agent for Au Metallic-NPs, might act as a 'molecular linker', which could help in the particle formation.[43]

2.4. SOLUTION NMR SPECTROSCOPY

Has been extensively used also for the characterization of oxide nanoparticle systems. Kahn and co-workers characterized ZnO Metallic-

NPs by 1 H and DOSY-NMR. They emphasized on the ability of the latter technique to sort species according to their size, as the diffusion coefficient is inversely proportional to the hydrodynamic radius. Their study, performed on ZnO Metallic-NPs stabilized by amine molecules, showed that a fast exchange between free and coordinated amine molecules was deduced within the NMR measurement timescale. Overall, the NMR spectra showed that the seemingly simple stabilization of ZnO Metallic-NPs by amine molecules appeared to be much more complicated than considered beforehand.[44]The same group published a study dedicated to the use of NMR techniques for the investigation of the role of amine ligands together with oleic acid on the formation of ZnO NP superlattices in C7D8. Their experiments demonstrated the dependence of the type of ligand adsorbed on the NP surface on the concentration of the colloidal NP solutions. It was suggested that the driving force of the superlattice formation was the presence of ion-paired ammonium carboxylate shells around each particle.[45]Yarger and colleagues investigated phosphonic acid-capped SnO2 Metallic-NPs with sizes lower than 5 nm, using multinuclear solution and solid-state magic angle spinning (MAS) NMR. The latter technique indicated the absence of acidic protons of the phosphonic acid groups, strongly supporting the formation of P–O–Sn linkages. Insights into the ligand structure and the extent of phosphonic acid protonation upon binding the NP surface were obtained.[46]In the case of Ca2SnO4 Metallic-NPs prepared by the mechanochemical synthetic route, Sn MAS-NMR and Sn Mössbauer were employed to probe the local environment of Sn nuclei, so as to acquire important insights into the local structural disorder of these Metallic-NPs. NMR spectroscopy provided information on the magnetic and chemical interactions, while Mössbauer measurements revealed the quadrupolar interactions experienced by the nuclei of Sn.[47]

2.5.   SOLID-STATE NMR (SS NMR) SPECTROSCOPY

It is an important characterization tool to investigate the behaviour of solid catalysts and chemical processes occurring at their surface. Such technique may help to resolve not only interactions at the ligand–solvent interface but also result in the acquisition of significant insight into ligand–particle bonding at the hard– soft matter interface.[33]For example, 31P is a very sensitive NMR nucleus with 100% natural abundance and high gyromagnetic ratio and it is quite easy to measure the 31P NMR spectra with a good signal

to noise ratio even in systems with low ligand concentrations. J-resolved 31P solid-state NMR spectroscopy combined with DFT calculations can provide important information about the structure of heterogenized species and also provide insights into the immobilization of homogeneous metal phosphine catalysts. Gutmann and co-workers have highlighted the crucial role of liquid and partly solidstate NMR techniques for the detection of surface molecules and the discrimination between different binding sites on nanoscale catalysts.[48]In particular, 2 H MAS NMR has been employed to study chemical reactions such as the hydrogenation of olefins, being capable of detecting reactive intermediates. The authors denoted a weakness of the NMR measurements, which was related to their sensitivity. Solid state 31P NMR was used to characterize phosphinine-stabilised Au Metallic-NPs and a phosphinine–Au complex, as reported by Mallissery and Gudat.[49]NMR spectra showed that in addition to metalbound intact phosphinine units, several surface-bound species generated by the chemical transformation of the initially supplied ligands were also detected. In another work, two different tripeptides attached on Au Metallic-NPs were analysed by SS NMR and DFT calculations. Substantial structural differences between CysAlaAla and AlaAlaCys on Au Metallic-NPs were evidenced through the aforementioned techniques. In particular, the location of the carboxylate moiety relative to the S atom that served to anchor the peptide to the surface played a significant role in determining these structures.[50]Novio et al. have used SS NMR and FTIR to characterize the location and dynamics of carbon monoxide coordination on Ru Metallic-NPs. Two different sets of 2 nm Ru Metallic-NPs were tested, prepared under a H2 atmosphere, stabilized by either PVP or a bidentate phosphine ligand (dppb). It was demonstrated that CO groups were mobile on the NP surface, while the bulky ancillary ligand dppb slowed down the fluxionally of CO and prevented the exchange at certain positions.[51]Lara et al. decomposed [Ru(COD) (COT)]   [(1,5-cyclooctadiene)(1,3,5-cyclooctatriene)ruthenium and [Pt(CH3)2(COD)] [dimethyl(1,5-cyclooctadiene)platinum(II)] organometallic complexes to produce small core–shell RuPt Metallic-NPs in the presence of PVP at room temperature. Several characterization techniques were combined for determining the structural composition of the particles, and 13CO was used for adsorption as a probe molecule. FTIR and SS NMR results were in agreement with the coordination of CO to Pt and in this way the

presence of a segregated Ru core/Pt shell structure was indicated. Measurements by WAXS, HRTEM, EXAFS and other techniques corroborated these findings.[52]

IV. MASS SPECTROMETRY (MS)

MS has drawn interest as a strong tool for the analytical characterisation of Metallic-NPs in a reliable way. MS offers invaluable elemental and molecular information on the composition, structure and chemical state of Metallic-NPs, and their bio-conjugation to target biomolecules. Furthermore, it can be used for bioconjugation quantification, as explained by Montoro Bustos et al. in ref. [53]. MS is compatible with any type of sample, apart from being a highly sensitive technique. In addition, it is easily coupled with separation techniques to obtain real-time information. In this way, varied and novel insights into the nature of Metallic-NPs and their final uses and applications can be potentially acquired.

2.6. INDUCTIVELY COUPLED PLASMA MS (ICP-MS)

ICP-MSis used for the elemental analysis of Metallic-NPs. It is characterized by robustness, high sensitivity and wide dynamic range, as well as high selectivity and virtual matrix independence. In addition, it is straightforward, usually requiring simple calibration protocols. It allows the reliable quantification and elemental composition characterisation of metallic-NPs, and it can determine metallic impurities in non metallic NPs. Molecular MS techniques, e.g. with electrospray ionisation (ESI) and matrix-assisted laser desorption/ionisation (MALDI), can provide information on the protecting ligands that surround the Metallic-NPs and also correlate the entire clusters with their chemical composition. Moreover, coupling size-exclusion chromatography with ICP-MS helps to gain information on the size distribution of Au Metallic-NPs and their elemental characterization. Certain characterization techniques, including capillary electrophoresis, hydrodynamic chromatography, ion mobility spectrometry and field flow fractionation (FFF), also offer useful information about the size and size distribution of Metallic-NPs. They can be coupled with ICP-MS, for example, FFF-ICP-MS can study the multi-elemental composition and size distribution of natural colloids.

2.7. SINGLE PARTICLE OPERATION MODE ICP-MS

The use of groundbreaking 'single particle operation mode' ICP-MS (spICP-MS) has helped to identify the concentration and size distribution of Metallic-NPs. In that case, highly diluted sample NP suspensions should be used for their characterisation. McLean and colleagues have written a review article on the characterization of thiolate-capped Au Metallic-NPs by mass spectrometry.[54]They reported that apart from characterizing the stabilising ligands and the elemental composition of the Metallic-NPs, they can also measure the core size and molecular stoichiometry. MS is a formidable tool for elucidating the size distribution of small clusters. It can also observe ligand mixtures with discrete stoichiometry.[54]Other techniques, such as NMR spectroscopy, can give population averages, providing only the percentage coverage of different thiolate ligands on an average nanoparticle. For instance, regarding Au Metallic-NPs, ICP-MS considers the gold core to be of constant mass. This allows the study of the variations in the stoichiometry of distinct ligands on the basis of mass in the following manner: if one characterizes gold Metallic-NPs containing mixed ligands with ICP-MS, he/she compares ligands of distinct masses and each population of ligands will correspond to a unique mass. This allows the differentiation between the distinct ligands in the cases of Metallic-NPs capped with more than one ligand.[55]

ICP-MS can also determine the size distribution and number concentration of Metallic-NPs in a single, fast analysis. It strongly depends on the matrix of the sample solution.[56]Regarding its capacity for the size characterisation of Au Metallic-NPs, Helfrich et al. have published a relevant article.[57]They presented an on-line coupling of liquid chromatography or gel electrophoresis with ICP-MS for the size determination and compared the results with other techniques. In particular, they mentioned that DLS is generally expected to give higher values than other techniques because the measured parameter is the hydrodynamic radius of the nanoparticle, but the results obtained by TEM provide information about the diameter of the Au core. Their results illustrated that the performance of on-line GE-ICP-MS is strongly related to the chemical structure of the NP surface composition. Good agreement was found between the different methods used for the size determination of their Au Metallic-NPs.[57]As mentioned before, the possibility to measure the size of Au Metallic-NPs was also demonstrated using spICP-MS. It has to be noted that for this determination, the chemical composition, density and shape of the Metallic-NPs are needed to be

known. Winchester and co-workers illustrated that precise size measurements by spICP-MS in the range of 20–200 nm can be achieved by operating the ICP-MS instrument in reduced sensitivity modes using a lower extraction voltage, collision cell/KED or higher mass resolution.[58] In addition, spICP-MS can detect and quantify the dissolved and nanoparticulate forms of Au at the same time. The detection of Au Metallic-NPs by the method in discussion is straightforward, but accurate measurement requires careful experimental design and data interpretation. The characterization of complex, polydisperse NP suspension by spICP-MS will require careful experimental design and data interpretation. Pace et al. also used spICP-MS to count and size Metallic-NPs. They mentioned the abovewritten advantages of the former method, but they also presented its drawbacks and future challenges. A major hurdle with spICP-MS is the improvement of the size detection limit. For multi-element particles and less ideal systems, spICP-MS may struggle to detect and size particles within the nanoscale range.[59] spICP-MS was also employed by Yang and co-workers to analyse Ag and Au Metallic-NPs in environmental water. The size distribution of these Ag and Au dispersions was in accordance with the TEM results.[60]

Besides, thiol ligand density was quantified at self-assembled monolayers on Au Metallic-NPs by ICP-MS. Gold and sulfur concentrations could be determined simultaneously by ICP-MS, and were obtained as ensemble averages of the particle distributions, as shown by Lammerhofer and colleagues.[61] The surface coverage of Au Metallic-NPs was studied quantitatively based on the linear relationship of the gold/sulfur (Au/S) ratio measured by ICP-MS, and the Au NP size measured by TEM. Their method proved to be a valuable tool for the quantification of ligand densities on the surface of Au Metallic-NPs. spICP-MS was also employed combined with tissue extraction for the quantification and characterization of PVP-capped Au and Ag Metallic-NPs in environmentally relevant biological tissues.[62] The authors described a size detection limit of 20 nm for these Ag and Au Metallic-NPs, but they noted that this value depends on instrument sensitivity and the ionic background for the metal of interest.

spICP-MS was also employed to characterize TiO2 and Au Metallic-NPs during water purification, in addition to the Ag Metallic-NPs. Parameters such as the NP concentration, size, size distribution and dissolved metal element concentration in surface water as well as in purified water were evaluated. Understanding the fate of Ti, Ag and Au during real potable water treatment processes is important since human exposure to these Metallic-NPs will eventually occur by drinking water. Donovan and co-workers found that lime softening followed by alum coagulation in combination with powdered activated carbon adsorption resulted in the complete removal of Au and Ag Metallic-NPs and almost complete removal of TiO2 Metallic-NPs.[63] The presence of titania Metallic-NPs was also investigated in sunscreens, using spICP-MS. The aforementioned parameters were studied (size, size distribution and NP concentration), and the developed method was considered of high throughput, reproducible, lowcost and sensitive.[64] The method under discussion has also been applied to detect lanthanide metals doped into the iron cores of superparamagnetic iron oxide Metallic-NPs in tissue and blood samples. With spICP-MS, more than 10 different NP formulations with distinct physicochemical properties could be directly analysed at the same time. As a proof of concept, their approach was used to study the influence of NP size and surface charge on tumor delivery, biodistribution and blood clearance in vivo. [65]

2.8. SECONDARY ION MASS SPECTROMETRY (SIMS)

SIMS is a mass spectral technique which can be used to obtain molecular chemical information from Metallic-NPs. It is a surface analysis technique where primary ions, which can be atomic or polyatomic, are used to sputter positively and negatively charged secondary ions. The secondary ions (SIs) originate from the outmost nanometer of the sample.[66] SIMS is in particular suitable for the analysis of Metallic-NPs by virtue of detection sensitivity and lateral (~100 nm) and depth (~1 nm) resolution. It is worth mentioning that the secondary ion signature of Metallic-NPs may be distinct in comparison with the one of bulk materials having the same composition. However, it is necessary to have a well-working methodology to deconvolute the analytical results.[67] Blanc et al. used SIMS to analyse the composition of dielectric Metallic-NPs localized in a silica glass matrix in the core of optical fibers. They performed SIMS imaging at high spatial resolution (NanoSIMS 50L) and their goal was to gain more understanding on the spectroscopic properties of the luminescent ions in these fibers. The authors mentioned that in SIMS the depth resolution is much better than the lateral resolution, which is related to the size of the probe.

The partitioning of P, Mg and Er into phase-separated zones was demonstrated, and this indicated that the particle composition was related to the Mg concentration. [68]

2.9. TIME OF FLIGHT SECONDARY ION MASS SPECTROMETRY (TOF-SIMS)

ToF-SIMS is a material characterisation technique that possesses high chemical sensitivity, high surface sensitivity (upper 2–3 nm probed) and molecular specificity. This method can analyse the nanoparticle drug delivery formulations.[69]In fact, ToF-SIMS is extensively used to characterize the nano-zones of larger components, such as electronic devices and thin to ultrathin films of either organic or inorganic nature. The technique under discussion is also utile for the investigation of the surface coating or functional groups of Metallic-NPs, for example, to analyse peptides coupled to Au Metallic-NPs and multilayer plasma deposited organic coatings on Al2O3 Metallic-NPs. Laus and colleagues noted that SIMS can be destructive while conducting the analysis. Even though the ion dose maximum limit can be adjusted to tackle the molecule destruction issue, the Metallic-NPs tested may still undergo melting. These authors used SIMS for the depth profiling of certain types of Metallic-NPs (Au–SiO2 and Ag–SiO2 configurations) and they investigated the depth profiles for melting issues, combining their SIMS study with additional characterization by SEM imaging. In all cases, the interpretation of the SIMS depth profiles illustrated that melting took place, although it is possible that with ultralow energy Cs+ this effect was limited to its minimum.[70]

Metallic-NPs are adsorbed on a surface; the bombardment of the primary ions results in the desorption of molecules (Metallic-NPs or NP conjugates), which then results in the emission of secondary ions from the outermost 1–1.5 nm molecular layers. The secondary ions are fragments of adsorbed molecules: metallic Metallic-NPs have high secondary ion yields, whereas organic Metallic-NPs yield chemical-specific fragments that help to determine the surface ligands. Kim et al. mention that when ToF-SIMS is combined with several NP-based signal enhancing strategies, it can probe the functionalization of Metallic-NPs as well as their locations and interactions in biological systems. NP-based SIMS is important for label-free drug screening because signal-enhancing Metallic-NPs can be designed to directly measure the enzyme activity. It can also be employed to monitor ligand-exchange processes. The benefit of ToF-SIMS, compared to MALDI-MS (matrix-assisted laser desorption/ionization), is the straightforward analysis of targets without any matrix use. Therefore, ToF-SIMS provides molecular information about functional groups, molecular orientation and conformation as well as denatured species from chemicals and/or from biomolecules. It can also be used to gain information on the core composition of Metallic-NPs, apart from their surface. The types of Metallic-NPs usually probed by ToF-SIMS are popular in domains such as biosensing and bio-imaging. Nevertheless, the spatial resolution of ToF-SIMS is limited to only hundreds of nanometers and ToF-SIMS is not particularly sensitive to high mass fragments. For a higher sensitivity and higher spatial resolution for the ability to detect metals in organic matrices, ToF-SIMS can be coupled **with laser secondary neutral mass spectrometry (laser-SNMS).** High-resolution NanoSIMS can provide monoatomic and diatomic secondary ions with a better sensitivity and spatial resolution than ToF-SIMS.207 Rafati et al. used ToF-SIMS to investigate polymer microspheres for the controlled release of a therapeutic protein from an implantable scaffold. The ability of ToF-SIMS imaging to spatially image the polyvinyl alcohol (PVA) surfactant and protein adsorbed onto the surface of the microspheres was shown for the first time.[71]

2.10. MATRIX ASSISTED LASER DESORPTION/ IONIZATION (MALDI)

Moreover, with mass spectrometry techniques, the sample needs to undergo ionization and subsequent sorting based on the mass to charge ratio in magnetic and electric fields. The desorption and ionization process can be assisted by ablation with a high energy laser (matrix assisted laser desorption/ ionization, MALDI) or a salvo of inert gases (fast atom bombardment). MALDI-ToF MS can characterize very small Metallic-NPs as it can quantify many particles at a time leading to an improved estimate of dispersity. The size range of the particles that can be analysed is very large and highly sensitive. MALDI-ToF was successfully employed by Hyeon and co-workers to estimate the NP size of spherical Ag Metallic-NPs in 9-nitroanthracene. The size values matched well with the ones measured by TEM. It was shown that the method under discussion can be used as a generic methodology to estimate with high precision the size and size distribution of Metallic-NPs with several shapes and sizes.[72]MALDI-ToF was also employed to characterize colloidal Pt Metallic-NPs prepared by Navin et al. The particles analysed were in the 1–4 nm size range and they were

stabilized by PVP. Particle sizes determined from mass spectra were found to be in good accordance with those derived from TEM and XRD experiments.[73]Zhang et al. used high-performance liquid chromatography coupled with mass spectrometry for the analysis of ultrasmall Pd Metallic-NPs. Reverse-phase HPLC is expected to offer more accurate determinations of the catalytic, electronic, optical and toxicological properties of metal Metallic-NPs. Among several separation techniques, HPLC can be considered as an effective approach to isolate different metal NP species. The authors employed RP-HPLC to separate and analyse for the first time water-soluble DMF-Pd Metallic-NPs. The measurements by MALDI-ToF MS were in agreement with the chemical compositions of the fractions. The aforementioned technique is the most popular MS technique in determining the number of metal atoms of NP fractions. It is further anticipated that RP-HPLC combined with MS can be applied to investigate the growth mechanism of Pd Metallic-NPs.[74]

V. INDUCTIVELY COUPLED PLASMA OPTICAL EMISSION SPECTROMETRY (ICP-OES)

ICP-OES is a highly sensitive technique that can characterize the core Metallic-NPs and also their coating ligands. It can reach tracelevel concentrations, small changes in concentration can be identified, and multiple elements can be detected at the same time. Therefore, it can provide information on surface species conjugated on Au Metallic-NPs and quantify the ligand packing density.[75]In addition, ICP-OES offers a wide dynamic linear range and it is well reproducible. Magnetic solid phase extraction (MSPE) combined with ICP-OES has been used to identify chromium ions in environmental water samples.[76]In addition, trace amounts of Cr, Cu and Pb can also be spotted by the combination of the aforementioned techniques.[77]

VI. INDUCTIVELY COUPLED PLASMA ATOMIC EMISSION SPECTROSCOPY (ICP-AES)

ICP-AES is a spectral method used to determine very precisely the elemental composition of samples; it can also be used to quantify the elemental concentration with the sample. ICP-AES uses high-energy plasma from an inert gas like argon to burn analytes very rapidly. The color that is emitted from the analyte is indicative of the elements present, and the intensity of the spectral signal is indicative of the concentration of the elements that is present.

CP-AES works by the emission of photons from analytes that are brought to an excited state by the use of high-energy plasma. The plasma source is induced when passing argon gas through an alternating electric field that is created by an inductively couple coil. When the analyte is excited the electrons try to dissipate the induced energy moving to a ground state of lower energy, in doing this they emit the excess energy in the form of light. The wavelength of light emitted depends on the energy gap between the excited energy level and the ground state. This is specific to the element based on the number of electrons the element has and electron orbital's are filled. In this way the wavelength of light can be used to determine what elements are present by detection of the light at specific wavelengths.

As a simple example consider the situation when placing a piece of copper wire into the flame of a candle. The flame turns green due to the emission of excited electrons within the copper metal, as the electrons try to dissipate the energy incurred from the flame, they move to a more stable state emitting energy in the form of light. The energy gap between the excited state to the ground state (ΔE indictates the color of the light or wavelength of the light, where h is Plank's constant (6.626×10^{-34} m^{2}kg/s), and ν is the frequency of the emitted light.)

$$\Delta E = h\nu$$

The wavelength of light is indicative of the element present. If another metal is placed in the flame such as iron a different color flame will be emitted because the electronic structure of iron is different from that of copper. This is a very simple analogy for what is happening in ICP-AES and how it is used to determine what elements are present. By detecting the wavelength of light that is emitted from the analyte one can deduce what elements are be present.

Naturally if there is a lot of the material present then there will be an accumulative effect making the intensity of the signal large. However, if there were very little materials present the signal would be low. By this rationale one can create a calibration curve from analyte solutions of known concentrations, whereby the intensity of the signal changes as a function of the concentration of the material that is present.When measuring the intensity from a sample of unknown concentration the intensity from this sample can be compared to that from the calibration curve, so this can be used

to determine the concentration of the analytes within the sample[78]

VII. DYNAMIC LIGHT SCATTERING (DLS)

DLS is a widely employed technique to find the size of metallic-NPs in colloidal suspensions in the nano- and submicrometer ranges. The metallic-NPs dispersed in a colloidal solution are in continuous Brownian motion. DLS measures light scattering as a function of time, which combined with the Stokes–Einstein assumption are used to determine the NP hydrodynamic diameter (i.e., diameter of the NP and the solvent molecules that diffuse at the same rate as the colloid) in solution. In DLS, a relatively low NP concentration is needed so that a multiple scattering effect is avoided.[79]Lim et al. have reviewed the characterization of Metallic-NPs by DLS focusing in the case of magnetic particles. They present how various factors such as suspension concentration, particle shape, colloidal stability and surface coating of metallic-NPs influence the size value obtained by DLS measurements. A comparison between the results derived from DLS and other techniques, such as TEM and AFM, is performed and the origins for any discrepancies in the sizing, for either small or larger particles, are discussed, while the working size range for each technique is also given.[80]For example, for small-sized Metallic-NPs, the radius of curvature effect is the principal contributing factor for the large difference observed for the diameter measured by TEM and DLS. Middle-sized Fe_3O_4 Metallic-NPs capped with oleic acid and oleylamine seem to have size values that show the best match among DLS and TEM measurements. The authors highlight the use of DLS also for the measurement of the colloidal stability of Metallic-NPs. Moreover, DLS has been proven useful to monitor the transient behaviours of β-FeOOH nanorods: these structures self-assemble in a side-by-side fashion to form highly oriented 2-D nanorod arrays, eventually leading to the formation of 3-D layered architectures. Overall, the realtime screening of Metallic-NPs by DLS provides important insights into their aggregation process, since it measures quantitatively the size of the particle clusters formed. The sensitivity of DLS to large particles is crucial for its excellent diagnostic capability to detect aggregation. Nevertheless, the authors denote that careful analysis is required for the best possible interpretation of the DLS results as they are affected by the factors previously mentioned (shape, coating agents, etc.).[80]The advantages of DLS include its quick, easy and precise operation for monomodal suspensions and the fact that it is an ensemble measurement method, yielding a good statistical representation of each NP sample. It is highly sensitive and reproducible for monodisperse, homogeneous samples. A limitation of DLS is the necessary conditions for the particles to be in suspension and undergoing Brownian motion. Large particles scatter much more light and even a small number of large particles can obscure the contribution from smaller particles. Therefore, its resolution for polydisperse, heterogeneous samples is rather low. DLS requires transformative calculations with assumptions that must be taken into account when interpreting the data – particularly with polydisperse samples. Although DLS can sometimes measure anisotropic nanostructures, it generally assumes spherical shaped particles.[81]Overall, DLS measures the hydrodynamic radius accurately but lacks the resolution to detect small aggregates.

Grobelny and co-workers investigated the size and size distribution of polydisperse silver NP colloids using DLS and UV-Vis. Although DLS is more sensitive than UV-Vis, its usual drawback has to do with the difficulty in detecting the presence of smaller Metallic-NPs; in addition, the UV-Vis spectra did not contain any separate peaks for Metallic-NPs of different sizes. Therefore, the authors concluded that UV-Vis should not be used for size determination in the case of polydisperse samples. UV-Vis and DLS are low-cost and fast methods, but care is needed when interpreting their results, especially for the aforementioned types of samples, which do not contain a single NP population. Complementary measurements with AFM and TEM/SEM will be certainly needed for polydisperse samples.[82]Murdock et al. characterized a broad range of nanomaterials in solution using DLS and TEM, before assessing their in vitro toxicity. Metal and metal oxide Metallic-NPs, such as Al, Al_2O_3, SiO_2 and Cu Metallic-NPs, as well as carbon-based materials such as carbon nanotubes, were tested. DLS measurements showed that depending on the material examined, when the Metallic-NPs are in solution they do not necessarily retain their nanoscale size.[83]

VIII.   NANOPARTICLE TRACKING ANALYSIS (NTA)

Is a relatively new, but quickly adopted, technique that can measure NP size, and having a lower concentration detection limit compared to DLS. It utilises the properties of both light scattering and Brownian movement so as to acquire a NP size distribution of samples in liquid dispersion. The details of its operation principle and further technical information are provided by Hole et al.[84]That paper examined the reproducibility of results acquired by NTA by investigating a wide range of nanoparticle systems and size ranges, in different media. The measurements were performed in 12 distinct laboratories, aiming to obtain a wide database. Examples of the types of nanomaterials tested were Au, SiO2 and polystyrene Metallic-NPs, dispersed in water or in biological media. An important advantage that NTA offers in comparison with other size measurement techniques is that it is not biased toward larger Metallic-NPs or aggregates. Furthermore, its confirmed accuracy and reproducibility verified the suitability of NTA to determine the size populations of bimodal samples. The comparison between NTA and DLS was also examined by Jiskoot and colleagues, investigating standard polystyrene beads in the size range of 60–1000 nm.178 Physical mixtures of samples with different NP sizes were also evaluated. It was shown that NTA yielded precise values for the size distribution of both monodisperse and polydisperse samples. The average size values recorded by NTA were slightly smaller and more exact to the nominal ones than those obtained by DLS. Nevertheless, NTA is slower and has a somewhat more difficult operation mode compared to DLS. That study corroborated the above-mentioned findings of other researchers which mention that DLS results are not easily interpreted in the case of polydisperse samples, whereas NTA is able to identify two different sample populations in the same sample.[85]Overall, NTA tracks single particles, while DLS studies an ensemble of particles and it is strongly biased to the biggest particles, which are present in the sample. NTA was also studied by Hassellov and co-workers for its capacity to determine the size distributions and concentrations of Metallic-NPs in liquid samples. Apart from the differences among DLS and NTA, the authors concluded that NTA allows the measurement of large amounts of particles, compared to TEM. Therefore, the statistical confidence is increased and the absence of any particle changes because of the preparation mode of the specimen tested is ensured. Additionally, NTA can potentially use the intensity of light scattered by individual particles to discriminate particles composed of distinct materials within a given size range.[86]It is important to note that the sensitivity of NTA is related to the size and composition of the nanomaterials studied.

NTA has also been employed to analyse the capping efficiencies of several biomass-derived stabilizers of colloidal Ag suspensions in water. The NTA software identifies and tracks single Metallic-NPs that undergo Brownian motion and correlates the velocity of the movement with the NP size. For instance, bigger Metallic-NPs and heavy aggregates move with a slow speed, in comparison with smaller Metallic-NPs, which have less weight and move faster. It was found that a biorefinery-derived residual syrup acted as an efficient stabilizing agent for silver Metallic-NPs in solution.[87]Another use of NTA, presented by van Leeuwen and co-workers, is the determination of the refractive index which dictates the interaction between light and Metallic-NPs. Heterogeneous Metallic-NPs were tested, with sizes < 500 nm in suspension, and NTA was capable of discriminating between SiO2 and polystyrene beads on the basis of their different refractive indexes. The authors noted that NTA can overestimate the mean diameter of the beads in comparison with TEM. This was attributed to the uncertainty in the measured diffusion coefficient and to the difference between the hydrodynamic diameter measured by NTA and the physical diameter measured by TEM.[88]

IX.   ZETA POTENTIAL (Z-POTENTIAL).

The ζ-potential of a sample is a key indicator of the stability of colloidal dispersions. Highly positively or negatively charged particles tend to repel each other, thus forming stable colloidal solutions which show only minor trends to agglomerate. Such highly charged particles are related to pH values which are far from the so-called 'isoelectric point' of a solution which refers to the pH value at which the zeta potential is zero. On the other hand, a low value for the ζ-potential of a colloidal NP dispersion causes the flocculation of the colloids and it corresponds to values closer to the isoelectric point of the system. In general, colloids with values for the ζ-potential in the range of ±20–30 mV or higher are considered stable. This property can be tuned through the modification of the surface chemistry, so the stabilisation of the

colloidal suspension is obtained via electrostatic repulsion. The ζ-potential is influenced by the concentration of the suspension and composition of the solvent and other additives. Since DLS can also provide indications on the aggregation tendency of a sol, it can be combined with ζ-potential measurements for a more complete characterization.[89]Branda et al. employed DLS and ζ-potential studies (which in fact can be carried out in the same device with modern instruments) to analyse the influence of the exposure to growth media on the size and surface charge of silica-based Stöber Metallic-NPs. These techniques appeared to be valuable tools to investigate the fate of Metallic-NPs in biological environments. Compared to TEM and SEM, the above-mentioned techniques offer the benefit that the Metallic-NPs are not exposed to the risk of clustering during sample preparation because of solvent evaporation.[90]Dobson and colleagues synthesized and characterized ultra-small superparamagnetic iron oxide Metallic-NPs thinly coated with SiO2. The authors noted that characterizing the NP surface properties was important for the understanding of properties under physiological conditions and optimizing the conjugation chemistry. Surface charge was characterized by ζ-potential analysis. Acid washes using HNO3 reversed the ζ-potential of the Fe3O4 colloid and removed any remaining ammonium ions, but also caused the material to release Fe2+, converting magnetite to maghemite, with no reduction in particle size.[91]

X. X-RAY-BASED TECHNIQUES
2.11. X-RAY DIFFRACTION (XRD)
XRD is one of the most extensively used techniques for the characterization of NPs.Typically; XRD provides information regarding the crystalline structure, nature of the phase, lattice parameters and crystalline grain size. The latter parameter is estimated by using the Scherrer equation using the broadening of the most intense peak of an XRD measurement for a specific sample. An advantage of the XRD techniques, commonly performed in samples of powder form, usually after drying their corresponding colloidal solutions, is that it results in statistically representative, volume-averaged values. The composition of the particles can be determined by comparing the position and intensity of the peaks with the reference patterns available from the International Centre for Diffraction Data (ICDD, previously known as Joint Committee on Powder Diffraction Standards, JCPDS) database. However,

it is not suitable for amorphous materials and the XRD peaks are too broad for particles with a size below 3 nm.

Upadhyay et al. determined the average crystallite size of magnetite NPs using X-ray line broadening and it was found to be in the range of 9–53 nm. The broadening of XRD peaks was mainly caused by particle/crystallite size and lattice strains other than instrumental broadening.[92]The XRD-derived size is usually bigger than the so-called magnetic size, due to the fact that smaller domains are present in a particle where all moments are aligned in the same direction, even if the particle is single domain. On the contrary, the TEM-deduced size was higher than that calculated using XRD, for samples with very large particles; in fact, when the particle size is bigger than 50 nm, there is more than one crystal boundary on their surface. XRD cannot distinguish between the two boundaries; therefore the actual (TEM) size of certain samples can be in reality bigger than the 50–55 nm calculated by the Scherrer formula. Dai and co-workers prepared ultra-small Au NPs which were very likely to be more developed along the ⟨111⟩ direction (rather than the ⟨220⟩ one) as the peak corresponding to the former direction was much more intense in their XRD measurement.[93]Similarly, Li and colleagues noticed that after preparing copper telluride nanostructures with different shapes (i.e. cubes, plates, and rods), the relative intensities between the different XRD peaks varied in relation to the particle shape.[94]

2.12. X-Ray Absorption Spectroscopy (XAS)
XAS includes both extended X-ray absorption fine structure (EXAFS) and X-ray absorption near edge structure (XANES, also known as NEXAFS). XAS measures the X-ray absorption coefficient of a material as a function of energy. Each element has a set of characteristic absorption edges corresponding to the different binding energies of its electrons, giving XAS element selectivity. As a highly sensitive technique, EXAFS is a convenient way to identify the chemical state of species which may occur even in very low concentrations. Synchrotrons are usually needed to acquire XAS spectra; therefore it is not a routine or readily available technique. XANES probes the density of states of empty/partially filled electronic states by considering the excitation of an inner shell electron to those states that are permitted by dipole selection rules. Pugsley et al. used in situ XAS to examine the kinetics and mechanism of formation of germanium NPs upon the reaction of Mg2Ge and GeCl4.[95]Actually, the EXAFS experiments and TEM results indicated the

formation of GeO2 NPs along with the Ge NPs. The analysis of EXAFS yielded a first-neighbour Ge–Ge distance of 2.45 Å in good agreement with XRD. Moreover, Chen et al. applied in situ EXAFS for the inspection of structural changes around germanium atoms in GeO2 NPs. Surprisingly, they noticed that at high temperature GeS2 was formed as a product of the complete transformation of germanium dioxide, in the presence of a sulfur source.[96]Requejo and co-workers investigated the effects of sulfur–palladium interaction on the structural and electronic properties of alkyl thiol-capped Pd NPs. The XANES and EXAFS analyses of the atomic structure and electronic properties of these NPs showed that the sulfidation of Pd clusters caused by the capping thiol molecules took place not only on the surface but also in the bulk.[97]

2.13. ENERGY DISPERSIVE EXTENDED X-RAY ABSORPTION FINE STRUCTURE EXAFS

EXAFS helps to determine both structural and kinetic parameters in supported metal catalysts for reactions occurring on a timescale of a few seconds. Such a fast operation enables the aforementioned technique to be used at temperatures higher than 200 °C, which would hinder the use of surface enhanced Raman spectroscopy (SERS), as the latter technique is not that fast under such conditions. Even on a timescale of tens of milliseconds, energy dispersive EXAFS can be used as a quantitatively suitable in situ probe of the dynamics of quick phase change in supported nanoparticulate metal catalysts.[98]

Bugaev and colleagues determined with EXAFS parameters the atomic structure of PtCu NPs in PtCu/C catalysts. EXAFS is one of the most convenient techniques for the structural analysis of NPs with sizes lower than 10 nm. It possesses a high spatial resolution and provides information on the nearest environment of an atom in a compound in the absence of long-range order. The parameters derived in that study were partial coordination numbers, interatomic distances and Debye–Waller factors.[14] Moreover, Klasovsky and co-workers performed a physicochemical characterization of a new electron-conducting polymer (PANI) supported PtO2 catalyst by electron paramagnetic resonance (EPR), diffffuse reflectance FTIR spectroscopy (DRIFTS) and EXAFS. The importance of in situ/operando techniques was highlighted toward a better comprehension of the working oxidation catalyst.[99]

Ingham has written a comprehensive review describing what X-ray scattering techniques such as EXAFS, in situ XRD and small-angle X-ray scattering (SAXS) can offer in nanoparticle characterization.[100]Beale and Weckhuysen have reported how the ratio between coordination numbers varied as a function of shape, through the EXAFS data. Their study concerned a series of nanoscale structures with several shapes and fcc, hcp, or bcc structures, with a maximum isotropic diameter of 3 nm.[101]In the case of Pt–Ru nanoclusters, size could also be obtained from EXAFS analysis, due to the fact that the coordination number of nearest neighbours in NPs is a non-linear function of the particle diameter if the latter parameter lies below the range of 3–5 nm.[102]Sokolov and co-workers characterized their Pd NPs – synthesized by two separate routes – by X-ray reflectivity, EXAFS and electron microscopy. The EXAFS-deduced size was lower than the TEM one if a cuboctahedral fcc structural model of Pd NPs surrounded by thiol was assumed. Compared to bulk Pd, lattice expansion was noticed in all types of NPs, by both HRTEM and EXAFS.[103]

2.14. Small-Angle X-Ray Scattering (SAXS)

Similar to the XRD method presented above, the SAXS technique allows elastic scattering processes into a given solid angle to be run; however the detector in SAXS covers only small scattering angles (normally lower than 1°).[104]A scheme that illustrates an in situ setup which manages to record realtime SAXS/WAXS/UV–Vis measurements during the formation of Au NPs is displayed in Fig. 1. The pictured device conducts SAXS and WAXS and records the UV–Vis spectra at the same time in a given sample volume.[105]WAXS (wide-angle X-ray scattering) is similar to SAXS, but the distance between the sample and the detector is smaller and therefore diffraction maxima at larger angles are observed. The authors investigated the nucleation and growth kinetics of gold NPs as a function of parameters such as concentration, temperature, ligand ratio and solvent type. Stuhn and co-workers characterized extensively polystyrene-grafted SiO2 NPs, using techniques such as SAXS, SANS, DLS, TGA and TEM. Small angle neutron scattering (SANS) provided direct access to the static structure of the polymer layer. Both SAXS and SANS can be used to measure the particle size; in that report, SAXS gave a 25.6 nm value, while a 23.3 nm NP size was derived by SANS. Although SANS and SAXS are very similar in various aspects (e.g. SANS uses elastic neutron scattering), the advantages of SANS over SAXS include its sensitivity to light elements, the possibility of isotope labelling and the strong scattering by

magnetic moments.[106]The ligand shells on small ZnO NPs were characterized by a combined SANS/SAXS approach. Standard in situ methods such as UV-Vis and SAXS are sensitive only to the ZnO core; however SANS probes the organic stabilizer in dispersion thanks to the high sensitivity of neutrons to H2. In the work under discussion, both techniques allowed the determination of the size distribution of the cores of the NPs and the distribution of the stabilizer molecules (acetate shell) simultaneously in the native solution.[107]Typically, SAXS is used to determine the particle size, size distribution, and shape. Regarding size values, SAXS results are more statistically average than TEM imaging. Wang et al. employed SAXS to investigate the structural change of Pt NPs with temperature.[108]For certain temperatures, the size obtained by XRD was different from the corresponding SAXS value. This is because SAXS is sensitive to the size of the fluctuation region of electronic density, but XRD is sensitive to the size of the long-range order region. SAXS provides the actual particle size, while XRD yields the crystallite size. It is important to note that the different size values of SAXS and XRD are related to the growth mode of NPs during thermal treatment. The particle size acquired with SAXS was found to be a little bigger than that obtained from TEM. The reason is that Pt NPs were coated with PVP, and the scattering intensity due to the PVP coating cannot be easily removed.[108]It has to be noted that SAXS is a low resolution technique and in certain cases further studies by XRD and/or electron diffraction techniques are indispensable for the characterization of NPs. In fact, Ti et al.have written a lengthy review article dedicated to the role of SAXS for nanoparticle research.[109]

2.15. X-Ray Photoelectron Spectroscopy (XPS)

XPS is the most widely used analytical technique for surface chemical analysis, also employed for the characterization of nanoscale materials. Its underlying physical principle is the photoelectric effect. XPS is a powerful quantitative technique, useful to elucidate the electronic structure, elemental composition and oxidation states of elements in a material. It can also analyse the ligand exchange interactions and surface functionalization of NPs as well as core/shell structures, and it operates under ultra-high vacuum conditions. Nag and co-workers have published a review paper describing the role of XPS as an interesting means to study the internal heterostructures of NPs. For example, it has been used to investigate the environmentdependent

crystal structure tuning of metal chalcogenide NPs of various sizes.[110]It can also distinguish between core/shell and homogeneous alloy structures, and identify the bonding mode of ligands such as trioctylphosphine oxide (TOPO) onto the surface of metal chalcogenide NPs. For example, if TOPO bonds preferentially to the surface metal element, then the uncapped surface chalcogenide element may oxidize more easily upon exposure to air. In comparison with microscopy techniques, like TEM and TEM/EELS, which use lateral spatial resolution to identify elements in a direction vertical to the probing electron beam, XPS probes the composition of the material along the direction of the electron beam. Regarding core–shell NPs, Shard has published an article that reports a straightforward method to interpret the XPS data for such types of particles. It involves a direct and accurate empirical method to convert the XPS intensities into overlayer thicknesses, mostly suitable for spherical NPs.[111]As further advantages of XPS the author mentions that it provides the depth information, similar to the size of NPs (up to 10 nm depth from the surface) and it does not significantly damage the samples. Two drawbacks of XPS analysis are the preparation of samples (i.e. dry solid form is required without contamination) and the interpretation of data. In another study, the interaction of L-cysteine with naked Au NPs has been studied with XPS: that report aimed to provide experimental spectroscopic support to the kinetic models of catalyst deactivation, studying the role of low-coordinated Au atoms belonging to NP edges and corners.[112]Furthermore, Minelli and co-workers wrote an article on the analysis of protein coatings on Au NPs by XPS and liquid based particle sizing techniques. XPS is robust and useful to study proteins quantitatively, as well as peptides adsorbed at Au interfaces. It can also characterize the molecular interface of Au NPs. The chemical information from the NP surface analysed by XPS can be used to assess the thickness of NP coatings.[113]Smirnov et al. used the so-called Davis' method to determine the size of Au NPs in the planar model Au/C systems based on the data of XPS. The NP size values derived by XPS agreed well with those from the scanning tunneling microscope (STM) data, with the degree of similarity being related to the particle shape (e.g. sphere, hemisphere and truncated hemisphere).[114]Tunc et al. presented a simple method by applying an external voltage stress during the XPS analysis of Au@SiO2 NPs; their method facilitated the detection, location and identification of charges developed on surface

structures in a completely non-contact mode. Therefore, XPS provided information not only on the chemical identity but also on the dielectric properties of nanomaterials, by recording their charging/discharging behaviour.[115]In another work, Polzonetti and colleagues used synchrotron XPS and NEXAFS to study the interaction at the molecule–metal interface and ligand arrangement in the molecular shell of Au NPs capped by aromatic thiols. The experimental results of both techniques were supported by density functional theory (DFT) calculations, illustrating the presence of a hybrid system in which the metallic Au core was surrounded by a shell of aromatic thiol molecules, whose thickness could be assessed by XPS.[116]Castner and coworkers quantified the impact of nanoparticle coatings and non uniformities on XPS analysis, for the case of Au@Ag core–shell NPs. They analysed the benefits of a complementary approach using XPS, STEM and simulated electron spectra for surface analysis (SESSA) simulations to characterize the structure and composition of NPs with non ideal geometries.[117]For instance, STEM provided information concerning the metallic cores and shells, while XPS provided information regarding organic species and contaminants that were difficult to identify by STEM.

XI. MICROSCOPY TECHNIQUES FOR NP CHARACTERIZATION

2.16. Transmission Electron Microscopy
TEM is a microscopy technique that exploits the interaction between a uniform current density electron beam (i.e. the energies are usually within a range of 60 to 150 keV) and a thin sample. When the electron beam reaches the sample, part of the electrons are transmitted, while the rest are elastically or inelastically scattered.[118]The magnitude of the interaction depends on severalfactors, such as size, sample density and elemental composition. The final image is built with the information acquired from the transmitted electrons. As it is clear from the previous sections, size and morphology define the unique set of physical properties, such as optical, magnetic, electronic and catalytic, of Metallic-NPs, as well as their interaction with biological systems.[119–121]TEM is the most common technique to analyse nanoparticle size and shape, since it provides not only direct images of the sample but also the most accurate estimation of the nanoparticle homogeneity. Nevertheless, some limitations have to be considered when using this technique, such as

the difficulty in quantifying a large number of particles or misleading images due to orientation effects. When characterizing very homogeneous samples, other techniques that analyse larger amounts of NPs can provide more reliable results, such as SAXS for larger and spherical Metallic-NPs,[122]or XRD by exploiting the bordering of the XRD reflections and the Scherrer formula.[123]However, a previous analysis has to be performed to ensure sample homogeneity.

Nanoparticle properties not only depend on their size and morphology but also other factors, like interparticle distance.For instance, when two metal Metallic-NPs are brought in close proximity, their plasmons couple, red-shifting their plasmon band and changing their colour. Therefore, TEM has been used to characterize the nanoparticle aggregation for different biomedical applications, including (1) sensing and diagnostics,where the aggregation depends on the presence of a biomarker or analyte; (2) therapy, where the aggregation causes an increase of the nanoparticle therapeutic effect; and (3) imaging, where the aggregation improves the response signal.[124,125] In order to obtain reliable results, extra care should be taken for sample preparation, since an inadequate protocol can result in sample alteration or artefact creation,[126]e.g. aggregation during the drying of the colloid suspension. Thus,TEM is usually combined with other techniques that can measure larger numbers of particles, and require less sample preparation, such as UV-Vis and DLS.[127]In recent years strong control over the nanoparticle assembly has been achieved, and a controlled NP self-assembly can lead to welldefined NP superlattices. The systematic assembly of different nanocrystals yields new multifunctional structures that combine the features of the individual building blocks, as well as the rise of new and exciting properties.[128]TEM has been one of the techniques used to characterize the formation of different super-lattice nanocomposites, which can be isostructural to several atomic crystal systems.[129]These new three-dimensional arrays are made of different Metallic-NPs (e.g. quantum dots, metals and magnetic NPs), and their final structure and composition can be controlled by tailoring the colloid surface charge or directional bonding with DNA.

In the last few years, the scientific community has started to view Metallic-NPs as dynamic systems, where their structure and properties can evolve over time as they interact with their surroundings. Therefore, it is important to characterize their dynamic transformations in

order to optimize their performance in many applications. For instance, sunlight has been reported to aggregate Ag Metallic-NPs and decrease their cytotoxicity.TEM imaging showed that nanobridges were formed between the Metallic-NPs upon sunlight exposure.[130]these morphological changes combined with surface sulfidation affected the nanoparticle dissolution rate, which caused the toxicity to decrease.Furthermore, TEM and DLS have been used to study the biodegradation of the nanoparticle polymeric coating by bacteria. The loss of the particle coating caused colloidal aggregation,which affected their mobility and cytotoxicity.

Furthermore, traditional TEM cannot be used to study the growth of NPs in solution. Nevertheless, it can be used to characterize the formation of colloids from solid precursors. For example, TEM has been used to image the growth dynamics of copper NPs.[131]these were synthesized in a heating holder by reducing copper phyllosilicate platelets with hydrogen. The in situ visualization allowed the characterization of the phase transformation of copper as the reaction was progressing. Another use of NPs concerns the field of therapeutic carriers, since they can enhance the efficiency of drugs by improving their stability and cellular uptake.[132]Two main techniques are used to study the interaction between NPs and cells: TEM and CLSM.[133]Both techniques are complementary and frequently used together, since TEM provides higher resolution than any other imaging technique while CLSM allows the live cell imaging and fluorescent labelling of different cell components. NPs are internalized through endocytosis after interacting with cell membrane receptors, such as scavenger receptors.[134]However, in order to increase their therapeutic effect, NPs need to escape from the vesicles and be released into the cytoplasm. Thus, TEM has been used to assess the location of NPs within a cell. For instance, it was used to study the Au NP shape and size requirements for higher cellular uptake and later vesicle escape. As mentioned in an earlier section of this review, the aggregation of NPs can change their physical properties. Therefore, TEM has been applied to characterize the dispersion of NPs after their internalization. For example, Au NPs grafted with PEG were well dispersed, and in low proportions within the intracellular vesicles of macrophages, while non-grafted Au NPs mostly accumulated as aggregates in the vesicles.[135]An additional advantage of TEM is that it allows the assessment of the changes of subcellular structures caused by the NPs. For instance, apoptosis-related

vacuoles were observed in melanoma cells after magnetic field hyperthermia treatment with iron oxide NPs was applied.[31]this observation helped to understand the cell death pathways in response to magnetic field hyperthermia. Finally, TEM has also been employed to define the degree of penetration of NPs through different tissues, such as TiO2 NPs through the skin for sunscreen applications.[136]

2.17. HIGH-RESOLUTION TEM (HRTEM)

HRTEM is an imaging mode of transmission electron microscopy that uses phase-contrast imaging, where both transmitted and scattered electrons are combined to produce the image.[137]In comparison with traditional TEM imaging, HRTEM requires a larger objective aperture in order to employ the scattered electrons. Phase-contrast imaging is the technique with the highest resolution ever developed and allows the detection of the arrays of atoms in crystalline structures.

HRTEM provides important information on the nanoparticle structure; in particular, while conventional electron microscopies can provide the statistical assessment of NP morphology, they do not have enough resolution to image the single particle crystal structure. Thus, HRTEM has become the most common technique to characterize the internal structure of Metallic-NPs. For instance, HRTEM has been used to study the effect of ligands in the final structure of Pt Metallic-NPs grown by organometallic synthesis.[138]Similarly, it has been employed to observe that the Pd nanoclusters (sizes between 1 and 1.5 nm) synthesized by a different organometallic protocol are a mixture of four different structured crystals with comparable energy levels,[139]. Furthermore, HRTEM can distinguish between single crystal and polycrystalline anisotropic Au Metallic-NPs that present similar optical properties.[140]HRTEM also allows the characterization of structural transitions, such as the thermal transition from disordered face-centred cubic to ordered L10 in iron–platinum Metallic-NPs. This thermal-induced event yields Metallic-NPs with enhanced coercivity and larger magnetocrystalline an isotropy, which are necessary qualities to build permanent magnets.

The imaging of single crystals also offers the opportunity to identify structural defects that may explain the unusual properties.For instance, it had been reported that the lattice constant of CeO2 Metallic-NPs increased with decreasing particle size.396 Nevertheless, no explanation had been found for such abnormal behaviour. A later study using HRTEM showed that these changes were not

caused by either disclinations (line defects) or volume expansions in the high angle boundaries. Combining these results with the ones from Raman spectroscopy, the authors concluded that the lattice expansion was the result of an increased number of point defects at smaller particle sizes.[139]Even though HRTEM is a powerful technique, it is worth mentioning that the characterization of Metallic-NPs is not always feasible by this technique. Due to the random orientation of the crystals relative to the electron source, there may be directions where the atoms are not well aligned, resulting in complex images that cannot be directly used to define the structure.[139]

2.18. Electron Diffraction (Ed)/ Selected Area Electron Diffraction (SAED)

SAED is another important microscopy tool for the study of the crystal structure of Metallic-NPs. Experiments are usually performed in a TEM, or a scanning electron microscope (SEM) as electron backscatter diffraction. In these instruments, electrons are accelerated by an electrostatic potential in order to gain the desired energy and determine their wavelength before they interact with the sample to be studied. The periodic structure of a crystalline solid acts as a diffraction grating, scattering the electrons in a predictable manner. Working back from the observed diffraction pattern, it may be possible to deduce the structure of the crystal producing the diffraction pattern. Buffat discussed the use of electron diffraction and HRTEM to investigate multiply-twinned structures and dynamical events in metal Metallic-NPs. The author noted that measuring the shrinkage of the lattice space by XRD may be complicated, as instrumental parameters, reflection broadening due to a very small NP size and matrix effects can lead to unclear XRD results. With ED, particles are lying rather free on a substrate, lower material quantity is needed for the measurement, and correlation with direct images of the crystals is possible. However, the study of size effects in Au and Pt by ED requires a careful interpretation of its results due to the complex multiply-twinned or icosahedral-like structure that appears in Metallic-NPs to lower the total free energy.431 The SAED technique is limited by the fact that many Metallic-NPscontribute to the diffraction pattern because of the relatively large size of the illuminated area, making their individual study difficult. In the more modern 'nanodiffraction' technique, the area of the sample which contributes to the diffraction pattern is limited by the size of the electron probe, which in a field emission TEM can be as small as 0.1 nm. In a paper concerning decahedral Au Metallic-NPs, the 'nano diffraction' approach was employed enabling the study of single Metallic-NPs, but it was demonstrated that the beam convergence produced a loss of symmetry from 10- to 5-fold in the diffraction pattern of the Metallic-NPs.[141]Schamp and Jesser used ED to calculate interplanar spacings and other lattice parameters of Au Metallic-NPs. An improved calculation of such parameters allows a more precise determination of the anisotropic strains in the gold Metallic-NPs.[142]In another work, the origin of the 'forbidden' reflections present in the [111] and [112] electron diffraction patterns of triangular-flatthin Au Metallic-NPs was explained.[143]Regarding another noble metal, Ag, Smyslov and co-workers combined SAXS, ED and microscopy experiments to determine the size and phase composition of Ag Metallic-NPs in a gel film of bacterial cellulose. In that report, SAXS provided a reliable estimate of the size of the Metallic-NPsin the moisture-containing composite; ED and electron microscopy permitted the performance of phase analysis, obtain images of Metallic-NPs and visualize their arrangement in the composite matrix.[144]

2.19. Scanning Transmission Electron Microscopy (STEM)

In STEM, the electron beam is focused to a fine spot that is then scanned over the sample in a raster, unlike conventional TEM. The rastering of the beam across the sample makes STEM appropriate for techniques such as Z-contrast annular dark-field imaging (explained below) and spectroscopic mapping by energy dispersive X-ray (EDX) spectroscopy or electron energy loss spectroscopy (EELS). Using EDX or EELS spectroscopy in the STEM it is possible to obtain elemental maps that show features down to the atomic scale. For the proper operation of STEM, the experimental determination of the absolute cross section is very challenging, as electron donors of high dynamical range are required. This has hampered the application of the STEMbased technique to a broad range of particle sizes, as one would wish. Nevertheless, mass information can be acquired through STEM-based mass measurements if a known mass standard can be established. For the characterization of the 3D morphology of Metallic-NPs, STEM electron tomography (analysed later in this review) is a very powerful technique and has been successfully employed for embedded and stable Metallic-NPs. The main restriction of the method is the time needed to take full tomographs and this might exclude many electron beam sensitive samples from analysis. To

tackle that difficulty, Palmer and co-workers developed a 'single-shot' approach to a three-dimensional measurement problem, using Au Metallic-NPs as the model system.[145]Haigh and co-workers published a paper on the investigation of the limitations and optimisation of EDX tomography within a STEM, focusing on the application of the technique to characterize the 3D elemental distribution of bimetallic Ag-Au Metallic-NPs. A key question they worked on for EDX tomography was whether the characteristic X-ray intensity generated in the STEM meets the requirements for the constraints of a particular sample and detector geometry.444 Ag Metallic-NPs exposed to light and humic substances were investigated by a combination of high resolution STEM, EELS and UV-Vis techniques. This multimethod approached facilitated the acquiring of information on NP morphology, surface chemistry transformations and corona formation. Despite the signal loss, probably by dissolution, that was noticed, there was no direct evidence of oxidation from the STEM-EELS.[146]The Palmer group has reported that not many applications of quantitative STEM exist in nanomaterial characterization. Therefore, they demonstrated a new approach to quantify the imaging contrast in STEM using size-selected clusters. The nanoclusters used consisted of Pd (Z = 46) and Au (Z = 79).[147]Finally, Deiana et al. used STEM-EDX to investigate the core–shell structure of bimetallic Pd–Hg Metallic-NPs, which proved to be a crystalline core– shell structure, with a Pd core and a Pd–Hg ordered alloy shell. The ordered shell was considered to be responsible for the high oxygen reduction selectivity to H2O2. [148]

2.20. ATOMIC FORCE MICROSCOPY (AFM)

AFMis a microscopy technique capable of creating three-dimensional images of surfaces at high magnification. It was initially developed by Gerard Binning and Heinrich Rohrer at IBM in 1986.[149]AFM is based on measuring the interacting forces between a fine probe and the sample. The probe is a sharp tip and is coupled to the end of a cantilever, which is made of silicon or silicon nitride. When the AFM scans the sample, the cantilever gets deflected as a result of the attractive or repulsive forces between the tip and the sample surface. The bending is quantified by a laser beam that reflects on the cantilever back side. The forces are finally calculated by combining the information from the laser variation and the known cantilever stiffness. AFM can scan under three different modes depending on the degree of proximity between the probe and the sample, i.e. contact, non-contact and tapping mode (also known as intermediate or oscillating mode).[150]The latter is the most common when characterizing Metallic-NPs. However, it is very sensitive to the free amplitude of the oscillating tip.518 In addition, other parameters, such as tip curvature radius, and surface energy and elasticity of the nanoparticle, influence the final topological values. Nevertheless, these factors can be minimized by plotting the particle height against the free amplitude of the oscillating probe, providing more reliable results.[151]Alternatively, non-contact is preferred when the sample is very sensitive and can be influenced by the tip– sample forces.

AFM has the advantage that it does not require any surface modification or coating prior to imaging. Thus, the topological analysis of small Metallic-NPs (≤6 nm), such as ion-doped Y2O3, has been performed by AFM without any special treatment. Low density materials, which present poor contrast in electron microscopy, have also been characterized. For instance, AFM was used to understand the formation mechanism of uniform patchy and hollow rectangular nanoplatelets made of polymer mixtures.520 Side-by-side comparison between AFM and electron microscopies, i.e. SEM and TEM, showed that AFM provided comparable results when analysing NP sizes.[152–154]AFM has the advantage that images the sample in three dimensions and allows the characterization of the nanoparticle height. Furthermore, it has similar resolution to SEM and TEM, while costing much less and occupying smaller laboratory space. Nevertheless, AFM displays slower scanning times than any electron microscope. Alternatively, spectroscopic techniques, such as DLS and photon correlation spectroscopy (PCS), have also been used to characterize the nanoparticle size. DLS and AFM provided similar results when the sample analysed was monodisperse and uniform.[154]However, only AFM could properly characterize Metallic-NPs with bimodal distribution sizes.[155]

AFM and XRD were jointly used to characterize Ag NP films, where both techniques provided complementary information.[156]In particular, AFM allowed the characterization of the grain size and the nanoparticle coverage of the surface, while XRD identified the preferential growth direction of the particles. Interestingly, at higher NP coverage, AFM showed that the film was made of larger particle grains. Nevertheless, XRD indicated that the crystal size remained the same. This apparent contradiction suggested that

the larger particles were formed by coalescence of different crystals, yielding larger polycrystalline grains. It is worth mentioning that a densely packed nanoparticle film can be challenging to characterize by AFM, since part of the particles are hidden by their neighbours. Therefore, several algorithms have been developed to estimate the nanoparticle size from the visible part of the image. These algorithms can be applied to densely packed sphericaland non-spherical particles.[157]

2.21. Scanning Electron Microscopy (SEM)

SEM is a widely used method for the high-resolution imaging of surfaces that can be employed to also characterize nanoscale materials. SEM uses electrons for imaging, much as a light microscope uses visible light. Mazzaglia et al. combined field-emission SEM (FE-SEM) and XPS measurements to study supramolecular colloidal systems of Au Metallic-NPs/amphiphilic cyclodextrin. These two techniques provided important information on the morphology and nature of the interaction of (thiohexyl carbon chain) SC6NH2 and (thiohexadecyl carbon chain) SC16NH2 with Au Metallic-NPs onto the silicon surface[158]Sinclair and co-workers have reported that SEM and NanoSIMS can be employed to locate Au Metallic-NPs in cells. SEM analysis illustrated its superiority compared to NanoSIMS for the analysis of inorganic Metallic-NPs in complex biological systems. NanoSIMS has a lower spatial resolution of around 50 nm while SEM is able to achieve resolutions down to 1 nm. The particles tested were Raman-active Au–core Metallic-NPs and NanoSIMS resulted in somewhat blurred images in certain cases due to its limited resolution. However, NanoSIMS has the unique capability to differentiate between isotopes, although this is not relevant for the case of Au Metallic-NPs.[159]High-resolution SEM (HRSEM) was used by Goldstein et al. for the imaging of Au Metallic-NPs in cells and tissues. The straightforward visualization of metallic Metallic-NPs is assured with this technique, and the sample preparation is fast and easy. However, in case of biological specimens, the need to decrease charging artefacts might make metal coating necessary, thus increasing the risks of radiation damage for the samples. The advantage of HRSEM, compared to other imaging techniques, is the capacity to scale down and study the arrangements of nanometric elements in their wider context. It allows the study of the specific spatial arrangement of Metallic-NPs and thus the examination of possible interactions between them. The results of that study indicated

the potential of HRSEM as a relatively simple tool to qualitatively screen the factors that enhance Au Metallic-NPs penetration, through the skin barrier. It can be considered as a powerful and diverse tool for the study of the interactions between biological systems and metallic nanostructures.[160]In another report, SEM and AFM measurements were compared for the same set of Metallic-NPs, that is, SiO2 and Au Metallic-NPs on mica or silicon substrates. For example, AFM observations enabled the measurement of the height of a nano-object with sub-nanometric accuracy, but the lateral measurements (along the X and Y axes) had large errors because of the tip/sample convolution. In contrast to the AFM, SEM cannot provide any metrological information on the height of the Metallic-NPs; however, modern SEM can give decent measurements of their lateral dimensions. In fact, the measurements of nearly spherical SiO2 Metallic-NPs by using both techniques gave similar results, showing the coherency and complementarity of both instruments.[161]SEM can be operated in the transmission mode, i.e. through the technique called 'transmission in scanning electron microscope' (T-SEM) . In the transmission mode, advanced NP analysis can be carried out by gaining in-depth information as well as analysis of ensembles of Metallic-NPs. In a paper by Rades et al., the combination of complementary techniques as SEM, T-SEM, EDX and scanning Auger microscopy (SAM) was proven to be a powerful strategy for comprehensive morphological and chemical evaluation of the properties of individual silica and titania Metallic-NPs. On the other hand, methods such as SAXS, DLS, XPS, XRD and BET would be suitable to characterize only the ensembles of the Metallic-NPs, and not single particles. T-SEM allows a quick examination of the NP shape, though its lateral resolution is limited to NP sizes down to 5–10 nm. TEM provides images with better quality, but T-SEM can be easily combined with EDX for a fast check of the NP size and elemental composition.[162]Hodoroaba et al. proved that T-SEM imaging provides a size distribution that is slightly broader than that obtained by TEM. For small SiO2 Metallic-NPs, the precise delimitation of the particles in the T-SEM mode is definitely constrained by the lower spatial resolution achieved compared to that of conventional TEM. In addition, with the T-SEM, the surface layer of the particles might not be always easily detected.[163]The same author noted in another paper that the conventional SEM imaging mode could not detect the Metallic-NPs on the back side of the support film that was required for the

observations. Therefore, an explicit knowledge of the T-SEM operator is needed for the measurements. The authors observed that the obtained SiO2 NP size distributions by SEM and TSEM in their work and for various conditions agreed well with each other, within the associated measurement uncertainties.[164]In another report, 3D reconstruction by focused ion beam (FIB) cutting and SEM imaging were combined to comprehend the evolution of pore volume, pore shape and other parameters during the two-step sintering of ZnO Metallic-NPs. In this way, the sintering process at the nanoscale for such particles can be better understood.[165]Ni- and Cu-co-doped zinc oxide Metallic-NPs prepared by the co-precipitation method were investigated by Ashokkumar and Muthukumaran by microstructure, optical and FTIR measurements. The depicted shape by SEM was in good agreement with the mathematical determinations from XRD, whereas FTIR provided important information on chemical bonding.[166]

XII. CONCLUSION

This review described the role of several different techniques for the characterization of nanoscale materials. Through this comprehensive summary of NP characterization methods, we demonstrated the uses of each one of them, emphasizing on their advantages and limitations, as well as on explaining how they can be effectively combined and how they can complement each other. The acquisition of a full picture of the variety of features that are associated with a nanomaterial requires typically the use of numerous techniques, often needing to use more than one of them for evaluating well and completely even a single property. By presenting the role of each technique in a comparative way, our review will act as a robust guide, helping the scientific community to understand better the discussed topic. In this way, researchers will be helped for the choice of the most suitable techniques for their characterization, together with the ability to assess their use in a more precise manner. Of course, there are challenges in the scientific community for the further improvement of the accuracy and resolution of many techniques. Therefore, we finally hope that a careful reading of this review will help to identify which valuable techniques merit efforts for further technical improvements.

REFERENCES

[1]. Heiligtag FJ, Niederberger M. The fascinating world of nanoparticle research. Vol. 16, Materials Today. 2013.

[2]. Willems NIT. Roadmap Report on Nanoparticles. Methodology. 2005;(November).

[3]. You H, Yang S, Ding B, Yang H. Synthesis of colloidal metal and metal alloy nanoparticles for electrochemical energy applications. Chem Soc Rev. 2013;42(7).

[4]. Auffan M, Rose J, Wiesner MR, Bottero JY. Chemical stability of metallic nanoparticles: A parameter controlling their potential cellular toxicity in vitro. Vol. 157, Environmental Pollution. 2009.

[5]. Chandra R, Chawla AK, Ayyub P. Optical and structural properties of sputter-deposited nanocrystalline Cu 2O films: Effect of sputtering gas. J Nanosci Nanotechnol. 2006;6(4).

[6]. Bhattacharya R, Mukherjee P. Biological properties of "naked" metal nanoparticles. Vol. 60, Advanced Drug Delivery Reviews. 2008.

[7]. Narayanan R, El-Sayed MA. Shape-dependent catalytic activity of platinum nanoparticles in colloidal solution. Nano Lett. 2004;4(7).

[8]. Moura D, Souza MT, Liverani L, Rella G, Luz GM, Mano JF, et al. Development of a bioactive glass-polymer composite for wound healing applications. Mater Sci Eng C. 2017;76.

[9]. Gomez-Romero P. Hybrid organic-inorganic materials - in search of synergic activity. Adv Mater. 2001;13(3).

[10]. Shaikh SF, Mane RS, Min BK, Hwang YJ, Joo OS. D-sorbitol-induced phase control of TiO2 nanoparticles and its application for dye-sensitized solar cells. Sci Rep. 2016;6.

[11]. Gracias DH, Tien J, Breen TL, Hsu C, Whitesides GM. Forming electrical networks in three dimensions by self-assembly. Science (80-). 2000;289(5482).

[12]. Chen W, Cai W, Zhang L, Wang G, Zhang L. Sonochemical processes and formation of gold nanoparticles within pores of mesoporous silica. J Colloid Interface Sci. 2001;238(2).

[13]. Geethalakshmi R, Sarada DVL. Gold and silver nanoparticles from Trianthema decandra: Synthesis, characterization, and antimicrobial properties. Int J Nanomedicine. 2012;7.

[14]. Vijayakumar M, Priya K, Nancy FT, Noorlidah A, Ahmed ABA. Biosynthesis, characterisation and anti-bacterial effect of

plant-mediated silver nanoparticles using Artemisia nilagirica. Ind Crops Prod. 2013;41(1).

[15]. Bhumkar DR, Joshi HM, Sastry M, Pokharkar VB. Chitosan reduced gold nanoparticles as novel carriers for transmucosal delivery of insulin. Pharm Res. 2007;24(8).

[16]. Sýkora D, Kašička V, Mikšík I, Řezanka P, Záruba K, Matějka P, et al. Application of gold nanoparticles in separation sciences. Vol. 33, Journal of Separation Science. 2010.

[17]. Chung IM, Park I, Seung-Hyun K, Thiruvengadam M, Rajakumar G. Plant-Mediated Synthesis of Silver Nanoparticles: Their Characteristic Properties and Therapeutic Applications. Vol. 11, Nanoscale Research Letters. 2016.

[18]. AshaRani P V., Mun GLK, Hande MP, Valiyaveettil S. Cytotoxicity and genotoxicity of silver nanoparticles in human cells. ACS Nano. 2009;3(2).

[19]. Rajput N. METHODS OF PREPARATION OF NANOPARTICLES-A REVIEW. Vol. 7, International Journal of Advances in Engineering & Technology. 2015.

[20]. Thanh N.; Mahiddine, S. NTK. M. Mechanisms of Nucleation and Growth of Nanoparticles in Solution. Chem Rev. 2014;114(15):7610–30.

[21]. Koczkur Stefanos; Polavarapu, Lakshminarayana; Skrabalak, Sara E. KM. M. Polyvinylpyrrolidone (PVP) in nanoparticle synthesis. Dalton Trans. 2015;44(41):17883–905.

[22]. Wang Dehui; Xie, Shuifen; Xia, Xiaohu; Huang, Cheng Zhi; Xia, Younan YW. Synthesis of Silver Octahedra with Controlled Sizes and Optical Properties via Seed-Mediated Growth. ACS Nano. 2013;7(5):4586–94.

[23]. Kim Stephen T.; Song, Hyunjoon; Kuykendall, Tevye; Yang, Peidong FC. Platonic Gold Nanocrystals. Angew Chem Int Ed Engl. 2004;43(28):3673–7.

[24]. Nanocamposix(Nanocamposix.com). No Title. UV/Vis/IR Spectroscopy analysis of NPs. 2012.

[25]. Hendel Maria; Kettemann, Frieder; Birnbaum, Alexander; Rademann, Klaus; Polte, Jörg TW. In situ determination of colloidal gold concentrations with UV-vis spectroscopy: limitations and perspectives. Anal Chem. 2014;86(22):11115–24.

[26]. Paramelle Anton; Gorelik, Sergey; Free, Paul; Hobley, Jonathan; Fernig, David G. DS. A rapid method to estimate the concentration of citrate capped silver nanoparticles from UV-visible light spectra. Analyst. 2014;139(19):4855–61.

[27]. Haiss Nguyen T. K.; Aveyard, Jenny; Fernig, David G. WT. Determination of size and concentration of gold nanoparticles from UV-vis spectra. Anal Chem. 2007;79(11):4215–21.

[28]. Ray Bethany R.; de Rutte, Joseph; Pennathur, Sumita TR. L. Quantitative Characterization of the Colloidal Stability of Metallic Nanoparticles Using UV–vis Absorbance Spectroscopy. Langmuir. 2015;31(12):3577–86.

[29]. Desai Venu; Gupta, SanjeevK.; Jha, Prafulla K. RM. Size Distribution of Silver Nanoparticles: UV-Visible Spectroscopic Assessment. Nanosci Nanotechnol Lett. 2012;4(1):30–4.

[30]. Bindhu Vasant; Umadevi, M. MR. S. Synthesis, characterization and SERS activity of biosynthesized silver nanoparticles. Spectrochim Acta A Mol Biomol Spectrosc. 2013;115(NA):409–15.

[31]. Blanco-Andujar Daniel; Southern, Paul; Nesbitt, Stephen A.; Thanh, Nguyen T. K.; Pankhurst, Quentin A. CO. Real-time tracking of delayed-onset cellular apoptosis induced by intracellular magnetic hyperthermia. Nanomedicine (Lond). 2015;11(2):121–36.

[32]. Syed B, Karthik N, Bhat P, Bisht N, Prasad A, Satish S, et al. Phyto-biologic bimetallic nanoparticles bearing antibacterial activity against human pathogens. J King Saud Univ - Sci. 2019;31(4).

[33]. Marbella Jill E. LE. M. NMR Techniques for Noble Metal Nanoparticles. Chem Mater. 2015;27(8):2721–39.

[34]. Scheid D.; Winter, Tamara; Gutmann, Torsten; Dietz, Christian; Gallei, Markus DS. The pivotal step of nanoparticle functionalization for the preparation of functional and magnetic hybrid opal films. J Mater Chem C. 2016;4(11):2187–96.

[35]. Vowinkel Stephen; Gutmann, Torsten; Gallei, Markus SP. Free-Standing and Self-Crosslinkable Hybrid Films by Core-Shell Particle Design and Processing. Nanomater (Basel, Switzerland). 2017;7(11):390-NA.

[36]. Hens José C. ZM. A Solution NMR Toolbox for Characterizing the Surface

Chemistry of Colloidal Nanocrystals. Chem Mater. 2013;25(8):1211–21.

[37]. Uccello-Barretta Claudio; Balzano, Federica; Vanni, Letizia; Aiello, Federica; Jicsinszky, Laszlo GE. Water soluble heptakis(6-deoxy-6-thio)cyclomaltoheptaose capped gold nanoparticles via metal vapour synthesis: NMR structural characterization and complexation properties. Carbohydr Res. 2011;346(6):753–8.

[38]. Canzi Anthony A.; Kubiak, Clifford P. GM. Diffusion-Ordered NMR Spectroscopy as a Reliable Alternative to TEM for Determining the Size of Gold Nanoparticles in Organic Solutions. J Phys Chem C. 2011;115(16):7972–8.

[39]. Coelho Maria; Pereira, Maria do Carmo; Coelho, Manuel A. N.; Ivanova, Galya SCR. Structural characterization of functionalized gold nanoparticles for drug delivery in cancer therapy: a NMR based approach. Phys Chem Chem Phys. 2015;17(29):18971–9.

[40]. Sharma Robert E.; Bouchard, Louis-S. RT. Intramolecular Ligand Dynamics in d15-(PPh3)-Capped Gold Nanoparticles Investigated by 2H NMR. J Phys Chem C. 2011;115(8):3297–303.

[41]. Smith Lauren E.; Johnston, Kathryn A.; Hartmann, Michael J.; Crawford, Scott E.; Kozycz, Lisa M.; Seferos, Dwight S.; Millstone, Jill E. AM. M. Quantitative Analysis of Thiolated Ligand Exchange on Gold Nanoparticles Monitored by 1H NMR Spectroscopy. Anal Chem. 2015;87(5):2771–8.

[42]. Sharma Gregory P.; Solomon, Virgil C.; Zimmermann, Herbert; Schiffenhaus, Steven; Amin, Samrat A.; Buttry, Daniel A.; Yarger, Jeffery L. RH. NMR characterization of ligand binding and exchange dynamics in triphenylphosphine-capped gold nanoparticles. J Phys Chem C. 2009;113(37):16387–93.

[43]. Doyen Kristin; Bruylants, Gilles MB. UV-Vis and NMR study of the formation of gold nanoparticles by citrate reduction: observation of gold-citrate aggregates. J Colloid Interface Sci. 2013;399(NA):1–5.

[44]. Coppel Grégory; Pagès, C.; Chaudret, Bruno; Maisonnat, André; Kahn, Myrtil L. YS. Full Characterization of Colloidal Solutions of Long-Alkyl-Chain-Amine-Stabilized ZnO Nanoparticles by NMR Spectroscopy: Surface State, Equilibria, and

Affinity. Chemistry. 2012;18(17):5384–93.

[45]. Gharbi Florent; Mathieu, Paul; Amiens, Catherine; Collière, Vincent; Coppel, Yannick; Philippot, Karine; Fontaine, Laurent; Montembault, Véronique; Smiri, Leila Samia; Ciuculescu-Pradines, Diana KS. Alkyl phosphonic acid-based ligands as tools for converting hydrophobic iron nanoparticles into water soluble iron–iron oxide core–shell nanoparticles. New J Chem. 2017;41(20):11898–905.

[46]. Holland Ramesh; Agola, Jacob O.; Amin, Samrat A.; Solomon, Virgil C.; Singh, Poonam; Buttry, Daniel A.; Yarger, Jeffery L. GP. S. NMR Characterization of Phosphonic Acid Capped SnO2 Nanoparticles. Chem Mater. 2007;19(10):2519–26.

[47]. Šepelák Klaus-Dieter; Bergmann, Ingo; Suzuki, Shigeru; Indris, Sylvio; Feldhoff, Armin; Heitjans, Paul; Grey, Clare P. VB. A One-Step Mechanochemical Route to Core−Shell Ca2SnO4 Nanoparticles Followed by 119Sn MAS NMR and 119Sn Mössbauer Spectroscopy. Chem Mater. 2009;21(12):2518–24.

[48]. Gutmann Anna; Rothermel, Niels; Werner, Mayke; Srour, Mohamad; Abdulhussain, Safaa; Tan, Shulin; Xu, Yeping; Breitzke, Hergen; Buntkowsky, Gerd TG. Solid-state NMR concepts for the investigation of supported transition metal catalysts and nanoparticles. Solid State Nucl Magn Reson. 2013;55(NA):1–11.

[49]. Mallissery Dietrich SKG. Solid-state 31P NMR characterisation of phosphinine-stabilised gold nanoparticles and a phosphinine-gold complex. Dalton Trans. 2010;39(18):4280–4.

[50]. Karki Hong; Geise, Natalie R.; Wilson, Brendan W.; Lewis, James P.; Gullion, Terry IW. Tripeptides on Gold Nanoparticles: Structural Differences between Two Reverse Sequences as Determined by Solid-State NMR and DFT Calculations. J Phys Chem B. 2015;119(36):11998–2006.

[51]. Novio Karine; Chaudret, Bruno FP. Location and Dynamics of CO Co-ordination on Ru Nanoparticles: A Solid State NMR Study. Catal Letters. 2010;140(1):1–7.

[52]. Lara Marie-José; Lecante, Pierre; Fazzini, Pier-Francesco; Philippot, Karine; Chaudret, Bruno PC. Segregation at a small scale:

synthesis of core–shell bimetallic RuPt nanoparticles, characterization and solid state NMR studies. J Mater Chem. 2012;22(8):3578–84.

[53]. Bustos Jorge Ruiz; Sanz-Medel, Alfredo ARME. Mass spectrometry for the characterisation of nanoparticles. Anal Bioanal Chem. 2013;405(17):5637–43.

[54]. Harkness David E.; McLean, John A. KM. C. Characterization of Thiolate-Protected Gold Nanoparticles by Mass Spectrometry. Analyst. 2010;135(5):868–74.

[55]. Carney Jin Young; Qian, Huifeng; Jin, Rongchao; Mehenni, Hakim; Stellacci, Francesco; Bakr, Osman M. RP. K. Determination of nanoparticle size distribution together with density or molecular weight by 2D analytical ultracentrifugation. Nat Commun. 2011;2(1):335.

[56]. Allabashi W.; de la Escosura-Muñiz, A.; Liste-Calleja, L.; Merkoçi, Arben RS. ICP-MS: a powerful technique for quantitative determination of gold nanoparticles without previous dissolving. J Nanoparticle Res. 2008;11(8):2003–11.

[57]. Helfrich Wolfram; Bettmer, Jörg AB. Size characterisation of Au nanoparticles by ICP-MS coupling techniques. J Anal At Spectrom. 2006;21(4):431–4.

[58]. Liu Karen E.; MacCuspie, Robert I.; Winchester, Michael R. JM. Capabilities of Single Particle Inductively Coupled Plasma Mass Spectrometry for the Size Measurement of Nanoparticles: A Case Study on Gold Nanoparticles. Anal Chem. 2014;86(7):3405–14.

[59]. Pace Nicola J.; Jarolimek, Chad V.; Coleman, Victoria A.; Higgins, Christopher P.; Ranville, James F. HE. R. Determining Transport Efficiency for the Purpose of Counting and Sizing Nanoparticles via Single Particle Inductively Coupled Plasma Mass Spectrometry. Anal Chem. 2011;83(24):9361–9.

[60]. Yang Chen-Lu; Li, Haipu; Wang, Qiang; Yang, Zhaoguang YL. Analysis of silver and gold nanoparticles in environmental water using single particle-inductively coupled plasma-mass spectrometry. Sci Total Environ. 2016;563(NA):996–1007.

[61]. Hinterwirth Stefanie; Waitz, Thomas; Prohaska, Thomas; Lindner, Wolfgang; Lämmerhofer, Michael HK. Quantifying Thiol Ligand Density of Self-Assembled Monolayers on Gold Nanoparticles by Inductively Coupled Plasma–Mass Spectrometry. ACS Nano. 2013;7(2):1129–36.

[62]. Gray Jessica G.; Bednar, Anthony J.; Kennedy, Alan J.; Ranville, James F.; Higgins, Christopher P. EP. C. Extraction and analysis of silver and gold nanoparticles from biological tissues using single particle inductively coupled plasma mass spectrometry. Environ Sci Technol. 2013;47(24):14315–23.

[63]. Donovan Craig D.; Ma, Yinfa; Stephan, Chady; Eichholz, Todd; Shi, Honglan AR. A. Single particle ICP-MS characterization of titanium dioxide, silver, and gold nanoparticles during drinking water treatment. Chemosphere. 2015;144(NA):148–53.

[64]. Dan Honglan; Stephan, Chady; Liang, Xinhua YS. Rapid analysis of titanium dioxide nanoparticles in sunscreens using single particle inductively coupled plasma–mass spectrometry. Microchem J. 2015;122(NA):119–26.

[65]. Crayton Drew R.; Zaki, Ajlan Al; Cheng, Zhiliang; Tsourkas, Andrew SH. E. ICP-MS analysis of lanthanide-doped nanoparticles as a non-radiative, multiplex approach to quantify biodistribution and blood clearance. Biomaterials. 2011;33(5):1509–19.

[66]. Rajagopalachary Stanislav V.; Schweikert, Emile A. SV. Examination of individual nanoparticles with cluster SIMS. Surf Interface Anal. 2010;43(1–2):547–50.

[67]. Liang Michael J.; Verkhoturov, Stanislav V.; Schweikert, Emile A. C-KE. Mass Spectrometry of Nanoparticles is Different. J Am Soc Mass Spectrom. 2015;26(8):1259–65.

[68]. Blanc Christelle; Dussardier, Bernard WG. Composition of nanoparticles in optical fibers by Secondary Ion Mass Spectrometry. Opt Mater Express. 2012;2(11):1504–10.

[69]. D.scurr. Challenges and opportunities in nanoparticle analysis using ToF-SIMS.

[70]. Yang Martin P.; Gilmore, Ian S.; Morris, Richard J. H.; Dowsett, Mark; Boarino, Luca; Sparnacci, Katia; Laus, Michele LS. Depth Profiling and Melting of Nanoparticles in Secondary Ion Mass Spectrometry (SIMS). J Phys Chem C. 2013;117(31):16042–52.

[71]. Rafati Asme; Shakesheff, Kevin M.; Shard, Alexander G.; Roberts, Clive J.; Chen,

Xinyong; Scurr, David J.; Rigby-Singleton, S; Whiteside, Paul T.; Alexander, Morgan R.; Davies, Martyn C. AB. Chemical and spatial analysis of protein loaded PLGA microspheres for drug delivery applications. J Control Release. 2012;162(2):321–9.

[72]. Kim Hogeun; Hackett, Michael J.; Park, Jinkyung; Seo, Pilsun; Hyeon, Taeghwan BHC. Size Characterization of Ultrasmall Silver Nanoparticles Using MALDI-TOF Mass Spectrometry. Bull Korean Chem Soc. 2014;35(3):961–4.

[73]. Navin Michael E.; Somorjai, Gabor A.; Marsh, Anderson L. JK. G. Characterization of Colloidal Platinum Nanoparticles by MALDI-TOF Mass Spectrometry. Anal Chem. 2009;81(15):6295–9.

[74]. Zhang Zhongping; Zhang, Yan; Paau, Man Chin; Hu, Qin; Gong, Xiaojuan; Shuang, Shaomin; Dong, Chuan; Peng, Xiaoguang; Choi, Martin M. F. LL. High-performance liquid chromatography coupled with mass spectrometry for analysis of ultrasmall palladium nanoparticles. Talanta. 2014;131(NA):632–9.

[75]. Elzey De-Hao D.; Rabb, Savelas A.; Yu, Lee L.; Winchester, Michael R.; Hackley, Vincent A. ST. Quantification of ligand packing density on gold nanoparticles using ICP-OES. Anal Bioanal Chem. 2012;403(1):145–9.

[76]. Cui Man; Chen, Beibei; Hu, Bin CH. Chitosan modified magnetic nanoparticles based solid phase extraction combined with ICP-OES for the speciation of Cr(III) and Cr(VI). Anal Methods. 2014;6(21):8577–83.

[77]. Suleiman Bin; Peng, Hanyong; Huang, Chaozhang JSH. Separation/preconcentration of trace amounts of Cr, Cu and Pb in environmental samples by magnetic solid-phase extraction with Bismuthiol-II-immobilized magnetic nanoparticles and their determination by ICP-OES. Talanta. 2008;77(5):1579–83.

[78]. Scheffer A, Engelhard C, Sperling M, Buscher W. ICP-MS as a new tool for the determination of gold nanoparticles in bioanalytical applications. Anal Bioanal Chem. 2008;390(1).

[79]. Kato H. Size Determination of Nanoparticles by Dynamic Light Scattering. In: Nanomaterials: Processing and Characterization with Lasers. 2012.

[80]. Lim Swee Pin; Che, Hui Xin; Low, Siew Chun JY. Characterization of magnetic nanoparticle by dynamic light scattering. Nanoscale Res Lett. 2013;8(1):381.

[81]. M.wolfgang. Nanoparticle Size Analysis:A survey and review.

[82]. Tomaszewska E, Soliwoda K, Kadziola K, Tkacz-Szczesna B, Celichowski G, Cichomski M, et al. Detection limits of DLS and UV-Vis spectroscopy in characterization of polydisperse nanoparticles colloids. J Nanomater. 2013;2013.

[83]. Braydich-Stolle LK, Lucas B, Schrand A, Murdock RC, Lee T, Schlager JJ, et al. Silver nanoparticles disrupt GDNF/Fyn kinase signaling in spermatogonial stem cells. Toxicol Sci. 2010;116(2).

[84]. Hole Katherine; Hannell, Claire; Maguire, Ciaran Manus; Roesslein, Matthias; Suarez, Guillaume; Capracotta, Sonja; Magdolenova, Zuzana; Horev-Azaria, Limor; Dybowska, Agnieszka; Cooke, Laura; Haase, Andrea; Contal, Servane; Manø, Stein; Vennemann, Antje; PS. Interlaboratory comparison of size measurements on nanoparticles using nanoparticle tracking analysis (NTA). J Nanopart Res. 2013;15(12):2101.

[85]. Filipe Andrea; Jiskoot, Wim VH. Critical Evaluation of Nanoparticle Tracking Analysis (NTA) by NanoSight for the Measurement of Nanoparticles and Protein Aggregates. Pharm Res. 2010;27(5):796–810.

[86]. Gallego-Urrea Jani; Hassellöv, Martin JA. T. Applications of particle-tracking analysis to the determination of size distributions and concentrations of nanoparticles in environmental, biological and food samples. TrAC Trends Anal Chem. 2011;30(3):473–83.

[87]. Luque Manuel; Garcia, Angel; Lastres, Carmen; Campos, Rafael; Pineda, Antonio; Romero, Antonio A.; Yepez, Alfonso RO. Evaluation of biomass-derived stabilising agents for colloidal silver nanoparticles via nanoparticle tracking analysis (NTA). RSC Adv. 2013;3(19):7119–23.

[88]. van der Pol Frank A. W.; Sturk, Auguste; Nieuwland, Rienk; van Leeuwen, Ton G. EC. Refractive Index Determination of Nanoparticles in Suspension Using Nanoparticle Tracking Analysis. Nano Lett. 2014;14(11):6195–201.

[89]. Baldassarre Matteo; Ciccarella, Giuseppe FC. A predictive model of iron oxide nanoparticles flocculation tuning Z-potential

in aqueous environment for biological application. J Nanoparticle Res. 2015;17(9):377-NA.

[90]. Branda Brigida; Costantini, Aniello; Luciani, Giuseppina FS. Effect of exposure to growth media on size and surface charge of silica based Stöber nanoparticles: a DLS and ζ-potential study. J Sol-Gel Sci Technol. 2014;73(1):54–61.

[91]. Bumb Martin W.; Choyke, Peter L.; Fugger, Lars; Eggeman, Alexander S.; Prabhakaran, Dharmalingam; Hutchinson, J; Dobson, Peter J. AB. Synthesis and characterization of ultra-small superparamagnetic iron oxide nanoparticles thinly coated with silica. Nanotechnology. 2008;19(33):335601.

[92]. Upadhyay Kinnari; Pandey, Brajesh SP. Influence of crystallite size on the magnetic properties of Fe3O4 nanoparticles. J Alloys Compd. 2016;678(NA):478–85.

[93]. Yan Valeri; Mahurin, Shannon M.; Overbury, Steven H.; Dai, Sheng WP. Powder XRD analysis and catalysis characterization of ultra-small gold nanoparticles deposited on titania-modified SBA-15. Catal Commun. 2005;6(6):404–8.

[94]. 94. Li Reza R.; Gil, Pilar Rivera; Pelaz, Beatriz; Ibáñez, Maria; Cadavid, Doris; Shavel, Alexey; Alvarez-Puebla, Ramon A.; Parak, Wolfgang J.; Arbiol, Jordi; Cabot, Andreu WZ. CuTe Nanocrystals: Shape and Size Control, Plasmonic Properties, and Use as SERS Probes and Photothermal Agents. J Am Chem Soc. 2013;135(19):7098–101.

[95]. Pugsley Craig L.; Sella, Andrea; Sankar, Gopinathan; McMillan, Paul F. AJ. B. XAS/EXAFS studies of Ge nanoparticles produced by reaction between Mg2Ge and GeCl4. J Solid State Chem. 2011;184(9):2345–52.

[96]. Chen Quan; Wang, Wei; Mo, Guang; Jiang, L. N.; Zhang, Kunhao; Chen, Zhongjun; Wu, Ziyu; Wu, Zhonghua XC. Formation of Ge–S Bonds from AOT-Coated GeO2 Nanoparticles at High Temperature: An in Situ Heating EXAFS Investigation. Chem Mater. 2008;20(8):2757–62.

[97]. Ramallo-López Lisandro J.; Craievich, Aldo F.; Vicentin, F. C.; Marín-Almazo, M.; Jose-Yacaman, Miguel; Requejo, Félix G. JM. G. XAFS, SAXS and HREM characterization of Pd nanoparticles capped with n-alkyl thiol molecules. Phys B Condens Matter. 2007;389(1):150–4.

[98]. Newton Steven G.; Guilera, Gemma; Jyoti, Bhrat; Evans, John MA. F. Oxidation/reduction kinetics of supported Rh/Rh2O3 nanoparticles in plug flow conditions using dispersive EXAFS. Chem Commun (Camb). 2004;NA(1):118–20.

[99]. Klasovsky Jens; Brückner, Angelika; Bonifer, Marcus; Arras, Jürgen; Steffan, Martin; Lucas, Martin; Radnik, Jörg; Roth, Christina; Claus, Peter FH. Catalytic and Mechanistic Investigation of Polyaniline Supported PtO2 Nanoparticles: A Combined in situ/operando EPR, DRIFTS, and EXAFS Study. J Phys Chem C. 2008;112(49):19555–9.

[100]. Ingham B. X-ray scattering characterisation of nanoparticles. Crystallogr Rev. 2015;21(4):229–303.

[101]. Beale Bert M. AM. W. EXAFS as a tool to interrogate the size and shape of mono and bimetallic catalyst nanoparticles. Phys Chem Chem Phys. 2010;12(21):5562–74.

[102]. Frenkel AI. Solving the structure of nanoparticles by multiple-scattering EXAFS analysis. J Synchrotron Radiat. 1999;6(3):293–5.

[103]. Sun Anatoly I.; Isseroff, Rebecca; Shonbrun, Cheryl; Forman, Michelle; Shin, Kwanwoo; Koga, Tadanori; White, Henry; Zhang, Lihua; Zhu, Yimei; Rafailovich, Miriam; Sokolov, Jonathan YF. Characterization of palladium nanoparticles by using X-ray reflectivity, EXAFS, and electron microscopy. Langmuir. 2005;22(2):807–16.

[104]. Kumar CSSR, Hormes J, Leuschner C. Nanofabrication Towards Biomedical Applications: Techniques, Tools, Applications, and Impact. Nanofabrication Towards Biomedical Applications: Techniques, Tools, Applications, and Impact. 2005.

[105]. Chen Jan; Hauschild, Stephan; Rosenfeldt, Sabine; Dulle, Martin; Förster, Stephan XS. Simultaneous SAXS/WAXS/UV-Vis Study of the Nucleation and Growth of Nanoparticles: A Test of Classical Nucleation Theory. Langmuir. 2015;31(42):11678–91.

[106]. Kim Katrin; Mazurowski, Markus; Gallei, Markus; Rehahn, Matthias; Spehr, Tinka; Frielinghaus, Henrich; Stühn, Bernd CJ. S. Synthesis and characterization of polystyrene chains on the surface of silica nanoparticles: comparison of SANS, SAXS,

and DLS results. Colloid Polym Sci. 2013;291(9):2087–99.

[107]. Schindler Martin; Schmutzler, Tilo; Kassar, Thaer; Segets, Doris; Peukert, Wolfgang; Radulescu, Aurel; Kriele, Armin; Gilles, Ralph; Unruh, Tobias TS. A Combined SAXS/SANS Study for the in Situ Characterization of Ligand Shells on Small Nanoparticles: The Case of ZnO. Langmuir. 2015;31(37):10130–6.

[108]. Wang Xiqiang; Cai, Quan; Mo, Guang; Jiang, L. S.; Zhang, Kunhao; Chen, Zhe; Wu, Zhonghua; Pan, W. WH. C. In situ SAXS study on size changes of platinum nanoparticles with temperature. Eur Phys J B. 2008;65(1):57–64.

[109]. 109. Li Andrew J.; Lee, Byeongdu TS. Small Angle X-ray Scattering for Nanoparticle Research. Chem Rev. 2016;116(18):11128–80.

[110]. Sarma Pralay K.; Mukherjee, Sumanta; Nag, Angshuman DD. S. X-ray Photoelectron Spectroscopy: A Unique Tool To Determine the Internal Heterostructure of Nanoparticles. Chem Mater. 2013;25(8):1222–32.

[111]. Shard AG. A Straightforward Method For Interpreting XPS Data From Core–Shell Nanoparticles. J Phys Chem C. 2012;116(31):16806–13.

[112]. Caprile Albano; Falletta, Ermelinda; Della Pina, Cristina; Cavalleri, Ornella; Rolandi, Ranieri; Terreni, S.; Ferrando, Riccardo; Rossi, Michele; Floreano, Luca; Canepa, Maurizio LC. Interaction of L-cysteine with naked gold nanoparticles supported on HOPG: a high resolution XPS investigation. Nanoscale. 2012;4(24):7727–34.

[113]. Belsey Alexander G.; Minelli, Caterina NA. S. Analysis of protein coatings on gold nanoparticles by XPS and liquid-based particle sizing techniques. Biointerphases. 2015;10(1):019012-NA.

[114]. Smirnov Alexander V.; Bukhtiyarov, Andrey V.; Prosvirin, Igor P.; Bukhtiyarov, Valerii I. MY. K. Using X-ray Photoelectron Spectroscopy To Evaluate Size of Metal Nanoparticles in the Model Au/C Samples. J Phys Chem C. 2016;120(19):10426.

[115]. Tunc U. Korcan; Suzer, Sefik; Correa-Duatre, Miguel A.; Liz-Marzán, Luis M. ID. Charging/discharging of Au (core)/silica (shell) nanoparticles as revealed by XPS. J Phys Chem B. 2005;109(50):24182–4.

[116]. Battocchio Francesco; Mukherjee, Subhrangsu; Magnano, Elena; Nappini, Silvia; Fratoddi, Ilaria; Quintiliani, Maurizio; Russo, Maria Vittoria; Polzonetti, Giovanni CP. Gold nanoparticles stabilized with aromatic thiols: Interaction at the molecule-metal interface and ligand arrangement in the molecular shell investigated by SR-XPS and NEXAFS. J Phys Chem C. 2014;118(15):8159–68.

[117]. Wang Mark H.; Baer, Donald R.; Castner, David G. Y-CAE. Quantifying the Impact of Nanoparticle Coatings and Nonuniformities on XPS Analysis: Gold/Silver Core–Shell Nanoparticles. Anal Chem. 2016;88(7):3917–25.

[118]. Reimer L, Kohl H. Transmission Electron Microscopy Physics of Image Formation. Vol. 51, Springer series in optical sciences. 2008.

[119]. Daniel Didier M-CA. Gold nanoparticles: assembly, supramolecular chemistry, quantum-size-related properties, and applications toward biology, catalysis, and nanotechnology. Chem Rev. 2003;104(1):293–346.

[120]. Fock Lara K.; González-Alonso, David; Espeso, J.I.; Hansen, Mikkel Fougt; Varón, Miriam; Frandsen, Cathrine; Pankhurst, Quentin A. JB. On the 'centre of gravity' method for measuring the composition of magnetite/maghemite mixtures, or the stoichiometry of magnetite-maghemite solid solutions, via 57Fe Mössbauer spectroscopy. J Phys D Appl Phys. 2017;50(26):265005-NA.

[121]. Pan Sabine; Leifert, Annika; Fischler, Monika; Wen, Fei; Simon, Ulrich; Schmid, Günter; Brandau, Wolfgang; Jahnen-Dechent, Willi YN. Size-Dependent Cytotoxicity of Gold Nanoparticles. Small. 2007;3(11):1941–9.

[122]. Borchert Elena V.; Robert, Aymeric; Mekis, Ivo; Kornowski, Andreas; Grübel, Gerhard; Weller, Horst HS. Determination of Nanocrystal Sizes: A Comparison of TEM, SAXS, and XRD Studies of Highly Monodisperse CoPt3 Particles. Langmuir. 2005;21(5):1931–6.

[123]. Alexander Harold P. LK. Determination of Crystallite Size with the X-Ray Spectrometer. J Appl Phys. 1950;21(2):137–42.

[124]. Vilela María Cristina; Escarpa, Alberto DG. Sensing colorimetric approaches based on gold and silver nanoparticles aggregation:

chemical creativity behind the assay. A review. Anal Chim Acta. 2012;751(NA):24–43.

[125]. Perrault Warren C. W. SD. C. In vivo assembly of nanoparticle components to improve targeted cancer imaging. Proc Natl Acad Sci U S A. 2010;107(25):11194–9.

[126]. Mahl Jörg; Meyer-Zaika, Wolfgang; Epple, Matthias DD. Possibilities and limitations of different analytical methods for the size determination of a bimodal dispersion of metallic nanoparticles. Colloids Surfaces A Physicochem Eng Asp. 2011;377(1):386–92.

[127]. Albanese Warren C. W. AC. Effect of gold nanoparticle aggregation on cell uptake and toxicity. ACS Nano. 2011;5(7):5478–89.

[128]. Courty Alain; Albouy, P. A.; Duval, Eugène; Pileni, Marie-Paule A. M. Vibrational coherence of self-organized silver nanocrystals in f.c.c. supra-crystals. Nat Mater. 2005;4(5):395–8.

[129]. Shevchenko Dmitri V.; Kotov, Nicholas A.; O'Brien, Stephen; Murray, Christopher B. EV. T. Structural diversity in binary nanoparticle superlattices. Nature. 2006;439(7072):55–9.

[130]. Cheng Liyan; Lin, Shihong; Wiesner, Mark R.; Bernhardt, Emily S.; Liu, Jie YY. Toxicity Reduction of Polymer-Stabilized Silver Nanoparticles by Sunlight. J Phys Chem C. 2011;115(11):4425–32.

[131]. van den Berg Christian Fink; Gommes, Cédric; Chorkendorff, Ib; Sehested, Jens; de Jongh, Petra E.; de Jong, Krijn P.; Helveg, Stig RE. Revealing the Formation of Copper Nanoparticles from a Homogeneous Solid Precursor by Electron Microscopy. J Am Chem Soc. 2016;138(10):3433–42.

[132]. Petros Joseph M. RA. D. Strategies in the design of nanoparticles for therapeutic applications. Nat Rev Drug Discov. 2010;9(8):615–27.

[133]. Ostrowski Daniel; Boreham, Alexander; Holzhausen, Cornelia; Mundhenk, Lars; Graf, Christina; Meinke, Martina C.; Vogt, Annika; Hadam, Sabrina; Lademann, Jürgen; Rühl, Eckart; Alexiev, Ulrike; Gruber, Achim D. AN. Overview about the localization of nanoparticles in tissue and cellular context by different imaging techniques. Beilstein J Nanotechnol. 2015;6(1):263–80.

[134]. Cutler Evelyn; Mirkin, Chad A. JI. A. Spherical Nucleic Acids. J Am Chem Soc. 2012;134(3):1376–91.

[135]. Walkey Jonathan B.; Guo, Hongbo; Emili, Andrew; Chan, Warren C. W. CO. Nanoparticle size and surface chemistry determine serum protein adsorption and macrophage uptake. J Am Chem Soc. 2012;134(4):2139–47.

[136]. Gontier Maria Dolores; Bíró, Tamás; Hunyadi, János; Kiss, Borbála; Gáspár, Krisztián; Pinheiro, Teresa; Silva, João Nuno; Filipe, Paulo; Stachura, J.; Dabros, Wojciech; Reinert, Tilo; Butz, Tilman; Moretto, Philippe; Surleve-Bazeille, J.E. EY. Is there penetration of titania nanoparticles in sunscreens through skin? A comparative electron and ion microscopy study. Nanotoxicology. 2008;2(4):218–31.

[137]. Williams C. Barry DB. C. Transmission Electron Microscopy - Transmission Electron Microscopy. Vol. NA, NA. 2009. 179–260 p.

[138]. Cure Yannick; Dammak, Thameur; Fazzini, Pier-Francesco; Mlayah, Adnen; Chaudret, Bruno; Fau, Pierre JC. Monitoring the Coordination of Amine Ligands on Silver Nanoparticles Using NMR and SERS. Langmuir. 2015;31(4):1362–7.

[139]. Jose-Yacaman M.; Ascencio, J. A. MM-A. High resolution TEM studies on palladium nanoparticles. J Mol Catal A Chem. 2001;173(1):61–74.

[140]. Pallares Yusong; Lim, Suo H; Thanh, Nguy n T K; Su, Xiaodi RM. W. Growth of anisotropic gold nanoparticles in photoresponsive fluid for UV sensing and erythema prediction. Nanomedicine (Lond). 2016;11(21):2845–60.

[141]. Romeu José LD. R-G. Interpretation of the nano-electron-diffraction patterns along the five-fold axis of decahedral gold nanoparticles. Microsc Microanal. 2011;17(2):279–83.

[142]. Schamp W.A. CT. J. On the measurement of lattice parameters in a collection of nanoparticles by transmission electron diffraction. Ultramicroscopy. 2004;103(2):165–72.

[143]. Reyes-Gasga A.; Gao, Xiaoxia; Jose-Yacaman, Miguel JG-R. On the interpretation of the forbidden spots observed in the electron diffraction patterns of flat Au triangular nanoparticles. Ultramicroscopy. 2008;108(9):929–36.

[144]. Volkov Vera V.; Shtykova, Eleonora V.; Dembo, K. A.; Arkharova, Natalia A.; Ivakin, G. I.; Smyslov, R. Yu. VK.

Determination of the size and phase composition of silver nanoparticles in a gel film of bacterial cellulose by small-angle X-ray scattering, electron diffraction, and electron microscopy. Crystallogr Reports. 2009;54(2):169–73.

[145]. Young Ziyou; Chen, Yu; Palomba, Stefano; Di Vece, M.; Palmer, Richard E. NP. L. Weighing Supported Nanoparticles: Size-Selected Clusters as Mass Standards in Nanometrology. Phys Rev Lett. 2008;101(24):246103.

[146]. Römer Zhiwei; Merrifield, Ruth C.; Palmer, Richard E.; Lead, Jamie R. IW. High Resolution STEM-EELS Study of Silver Nanoparticles Exposed to Light and Humic Substances. Environ Sci Technol. 2016;50(5):2183–90.

[147]. Wang Ziyou; Park, S. J.; Abdela, A.; Tang, D.; Palmer, Richard E. ZL. Quantitative Z-contrast imaging in the scanning transmission electron microscope with size-selected clusters. Phys Rev B. 2011;84(7):073408-NA.

[148]. Deiana Arnau; Malacrida, Paolo; Stephens, Ifan E. L.; Chorkendorff, Ib; Wagner, Jakob Birkedal; Hansen, Thomas Willum DV-C. Determination of Core-Shell Structures in Pd-Hg Nanoparticles by STEM-EDX. ChemCatChem. 2015;7(22):3748–52.

[149]. Binnig Calvin F.; Gerber, Ch. G. Q. Atomic force microscope. Phys Rev Lett. 1986;56(9):930–3.

[150]. Vilalta-Clemente G.; Nouf-Allehiani, M.; Gamarra, Piero; di Forte-Poisson, M.A.; Trager-Cowan, Carol; Wilkinson, Angus J. AN-K. Cross-correlation based high resolution electron backscatter diffraction and electron channelling contrast imaging for strain mapping and dislocation distributions in InAlN thin films. Acta Mater. 2017;125(NA):125–35.

[151]. Mechler J.; Kokavecz, Janos; Hoel, Anders; Granqvist, Claes-Göran; Heszler, Peter AK. Anomalies in nanostructure size measurements by AFM. Phys Rev B. 2005;72(12):125407-NA.

[152]. Pitto-Barry Luís M. A.; Walker, Marc; Lawrence, James; Costantini, Giovanni; Sadler, Peter J.; Barry, Nicolas P. E. AP. Synthesis and controlled growth of osmium nanoparticles by electron irradiation. Dalton Trans. 2015;44(47):20308–11.

[153]. Hubenthal David; Träger, Frank FS. Determination of Morphological Parameters of Supported Gold Nanoparticles: Comparison of AFM Combined with Optical Spectroscopy and Theoretical Modeling versus TEM. Appl Sci. 2012;2(3):566–83.

[154]. Oćwieja Maria; Adamczyk, Zbigniew MM. Self-assembled silver nanoparticles monolayers on mica-AFM, SEM, and electrokinetic characteristics. J Nanopart Res. 2013;15(3):1460.

[155]. Hoo Natasha; West, Paul E.; Mecartney, Martha L. CM. S. A comparison of atomic force microscopy (AFM) and dynamic light scattering (DLS) methods to characterize nanoparticle size distributions. J Nanoparticle Res. 2008;10(1):89–96.

[156]. de Andrade Rogério; Macedo, Marcelo A.; Cunha, F. JEM. AFM and XRD characterization of silver nanoparticles films deposited on the surface of DGEBA epoxy resin by ion sputtering. Polímeros. 2013;23(1):19–23.

[157]. Fekete Kateřina; Petrak, Vaclav; Kratochvílová, Irena LK. AFM topographies of densely packed nanoparticles: a quick way to determine the lateral size distribution by autocorrelation function analysis. J Nanoparticle Res. 2012;14(8):1062-NA.

[158]. Mazzaglia Luigi Monsù; Mezzi, Alessio; Kaciulis, Saulius; de Caro, Tilde; Ingo, Gabriel Maria; Padeletti, Giuseppina AS. Supramolecular Colloidal Systems of Gold Nanoparticles/Amphiphilic Cyclodextrin: a FE-SEM and XPS Investigation of Nanostructures Assembled onto Solid Surface. J Phys Chem C. 2009;113(29):12772–7.

[159]. Kempen Chuck; Sasportas, Laura S.; Gambhir, Sanjiv S.; Sinclair, Robert PJ. H. Advanced Characterization Techniques for Nanoparticles for Cancer Research: Applications of SEM and NanoSIMS for Locating Au Nanoparticles in Cells. Mater Res Soc Symp Proc. 2013;1569(1):157–63.

[160]. Goldstein Yoram; Frušić-Zlotkin, Marina; Popov, I.; Kohen, Ron A. S. High resolution SEM imaging of gold nanoparticles in cells and tissues. J Microsc. 2014;256(3):237–47.

[161]. Delvallée Nicolas; Ducourtieux, Sebastien; Trabelsi, M.; Hochepied, Jean-François AF. Direct comparison of AFM and SEM measurements on the same set of nanoparticles. Meas Sci Technol. 2015;26(8):085601-NA.

[162]. Rades Vasile-Dan; Salge, Tobias; Wirth, Thomas; Lobera, M. Pilar; Labrador,

Roberto Hanoi; Natte, Kishore; Behnke, Thomas; Gross, Thomas; Unger, Wolfgang E. S. SH. High-resolution imaging with SEM/T-SEM, EDX and SAM as a combined methodical approach for morphological and elemental analyses of single engineered nanoparticles. RSC Adv. 2014;4(91):49577–87.

[163]. Hodoroaba Steffi; Unger, Wolfgang E. S. V-DR. Inspection of morphology and elemental imaging of single nanoparticles by high-resolution SEM/EDX in transmission mode. Surf Interface Anal. 2014;46(10–11):945–8.

[164]. 164. Hodoroaba C.; Macé, T.; Vaslin-Reimann, S. V-DM. Performance of high-resolution SEM/EDX systems equipped with transmission mode (TSEM) for imaging and measurement of size and size distribution of spherical nanoparticles. Microsc Microanal. 2014;20(2):602–12.

[165]. 165. Wang Y, Wan D, Xie S, Xia X, Huang CZ, Y. Xia AN. 7. 2013;4586.

[166]. 166. Ashokkumar S. MM. Microstructure, optical and FTIR studies of Ni, Cu co-doped ZnO nanoparticles by co-precipitation method. Opt Mater (Amst). 2014;37(NA):671–8.